1-1-2004

Factors influencing the efficiency of a moving bed granular filter

Joseph Allen Ritzert
Iowa State University

Factors influencing the efficiency of a moving bed granular filter

by

Joseph Allen Ritzert

A thesis submitted to the graduate faculty

in partial fulfillment of the requirements for the degree of

MASTER OF SCIENCE

Co-majors: Mechanical Engineering; Biorenewable Resources and Technology

Program of Study Committee
Robert Brown, Co-major Professor
Brent Shanks, Co-major Professor
Jon Van Gerpen

Iowa State University

Ames, Iowa

2004

Graduate College
Iowa State University

This is to certify that the master's thesis of

Joseph Allen Ritzert

has met the requirements of Iowa State University

Signatures have been redacted for privacy

TABLE OF CONTENTS

LIST OF FIGURES

LIST OF TABLES

ACKNOWLEDGEMENTS

I would like to express my appreciation to Dr. Robert Brown for the opportunity to conduct research under his supervision. His intellectual conversations have directed my research paths into new areas and have motivated me throughout this project. I also want to thank Daren Daugaard for introducing me to the pyrolysis system and for discussing important issues regarding my research.

I also extend my appreciation to Diane Love, Tonia McCarly, Jerod Smeenk, Sammy Sadaka, and the rest of the CSET team for their support during my research. I also want to thank Norm Olsen, Kirk Menges, Scott Munhall and Eric Denney for their support and efforts while helping to conduct the research at BECON.

I want to express my appreciation to Dr. Jon Van Gerpen and Dr. Brent Shanks for serving on my program of study committee and providing me with valuable insights and information regarding the investigation and preparation of my research and this thesis.

I want to thank my wife Amanda Ritzert for her loving support and encouragement during frustrating periods, and for allowing me to bring work home to get her opinion and providing technical writing support. I would also like to express appreciation to the rest of my family and friends for listening with concern and taking interest in my research.

ABSTRACT

The purpose of this research was to evaluate and optimize the performance of a moving bed granular filter (MBGF). A moving bed granular filter was constructed to test the removal of char particles from a high temperature product stream produced by a biomass pyrolysis system. Tests described in this thesis were performed under cold flow conditions.

Cold flow testing was designed to identify important physical parameters of the system that characterize filtration efficiency. Parameters such as gas velocity, bed depth, downcomer diameter, and granule size as well as dust characteristics were investigated. A correlation of bed depth and gas velocity has also been developed to allow design engineers to design a MBGF system based on known gas flow and dust conditions.

Experiments performed under cold flow testing with coal-derived fly ash verify levels of filtration efficiency exceeding 99% for some filter arrangements. However, char particles from the pyrolysis system do not filter as efficiently as fly ash due different particle properties such as particle size, surface roughness, shape, and density. Particles with high kinetic energy experience rebound from the granular surface, and consequently have low filtration efficiencies. Filtration efficiencies are high for particles that do not bounce and the granular filter system has high efficiencies for small particles in the pyrolysis system. A pre-filtration device should still be used in conjunction with the MBGF system to remove particulate with higher kinetic energy.

1. INTRODUCTION

The U.S. Department of Energy has written a vision and roadmap for the development of a biobased economy in the United States [1,2]. To reach the goals outlined in these documents, considerable research is being done on how to utilize biomass resources for efficient energy production. For the purposes of this research biomass is defined as woody or herbaceous plant material. The thermal conversion of biomass into liquid oil is called fast pyrolysis.

This research on fast pyrolysis uses a fluidized sand bed heated to 500°C in the absence of oxygen to decompose the biomass into aerosols and condensable vapors, non-condensable gases, and solid particulate or char. The char is then filtered from the product stream before the products are cooled and condensed by various methods. The condensed liquid is sometimes referred to as pyrolysis liquid or bio-oil. The end use applications of bio-oil require the efficient and economic removal of the char particles from the product stream. The char can be filtered from the condensed liquid, however the viscosity of the liquid makes this difficult. Thus, hot filtration of the product stream is highly desirable.

Due to temperatures exceeding 400°C and the liquid being acidic, traditional filters cannot withstand pyrolysis conditions. Conventional barrier filters become plugged with char particles and require shut down of the system for filter cleaning. The most widely used continuous filtration method uses cyclonic separators to collect char. The efficiency of cyclonic removal is limited by particle inertia and decreases rapidly as particle size decreases. When cyclones are designed to remove smaller particle sizes, the pressure drop required to force gas flow increases. Moving bed granular filters can have efficiencies exceeding 99%, and they can operate continuously at steady state under pyrolysis conditions with small pressure drop [3]. This research was conducted to investigate the mechanisms of moving bed granular filtration affecting the filtration of char in pyrolysis oil production.

2. BACKGROUND AND LITERATURE REVIEW

2.1 Fast pyrolysis

2.1.1 Definition

Fast pyrolysis is defined as the thermal decomposition of biomass in the absence of oxygen [4]. Biomass is heated to around 500°C in less than two seconds after entering a fluidized sand bed reactor. The heat causes a decomposition of the biomass into liquid aerosols, gases, and solid char. Fast pyrolysis utilizes short residence times in the reactor to optimize oil yield. This thermal conversion of biomass is a relatively new process compared to combustion and much research remains to make this process more useful and efficient. One aspect that requires more research is the removal of solid char from the pyrolysis oil. The moving bed granular filter has many characteristics favorable to fast pyrolysis, but its performance has not been optimized.

2.1.2 Pyrolysis filtration requirements

Char is commonly removed from the pyrolysis product stream by cyclones. The cyclones remove the char with efficiencies exceeding 95%, however efficiencies exceeding 99% are required for many of the desired bio-oil applications. The aerosols and gases are subsequently condensed and collected. The non-condensable gases that remain are re-circulated as a carrier gas or are used as heating fuel for the pyrolysis system.

The pyrolysis liquid that is collected can be more easily stored and transported than the biomass from which it was derived. It can be used as a substitute for fuel oil or diesel fuel in many stationary heating or electricity generating applications [4]. It can also be used as a source for other chemicals used in the chemical industry such as food flavorings, resins, fertilizers and agri-chemicals [4]. Other potential uses for bio-oil such as transportation fuels continue to be researched.

The current applications for bio-oil require that the solid char be removed to leave a pure liquid. For example, the presence of char in oil used in diesel engines causes excessive wear and clogging of fuel injection systems [5]. Char also catalyzes chemical reactions in the condensed oil that causes the viscosity to increase over time [5]. These reactions are not well understood, but removal of the char increases the oil stability allowing for it to be stored for longer periods of time. Collection of char on filter surfaces under hot conditions behaves as a cracking catalyst reducing heavier liquid and condensable gases down to non-condensable gases as they come into contact with the char [6]. Fast, efficient removal of char from the product stream is essential to reduce the interactions between char and the other pyrolysis products.

2.2 Granular filtration

2.2.1 Definition

Granular filtration is a fluid-solid separation process that removes suspended particulate from a flowing gas or liquid. The suspension flow is forced through a matrix of granular media typically described as a bed. As the dust laden product stream passes through the bed, various forces acting on the suspended particles cause them to interact with and become deposited on the surface of the granules [7].

Moving bed granular filters have been demonstrated to filter with efficiencies exceeding 99% [8], and the availability of various inert granular media make this a potential solution to bio-oil filtering needs. MBGF systems are increasingly important in the filtration of hot and corrosive gases where other filters cannot be used. It has also been noted that including sorbent material in with the media can be used to remove undesired compounds [9].

2.2.2 Basic principles and mechanisms of aerosol filtration

The performance of a granular bed filter is most commonly expressed as the particle collection efficiency (η), which is the weight ratio of the dust removed to the dust entering the filter. See **Appendix A** for a sample calculation of efficiency.

$$\eta = \frac{m_{in} - m_{out}}{m_{in}}$$

Particle collection efficiency is a function of many variables, but five main mechanisms act to remove particulate in granular beds and are discussed below [7]. **Figure 1** displays three of the five main mechanisms of filtration.

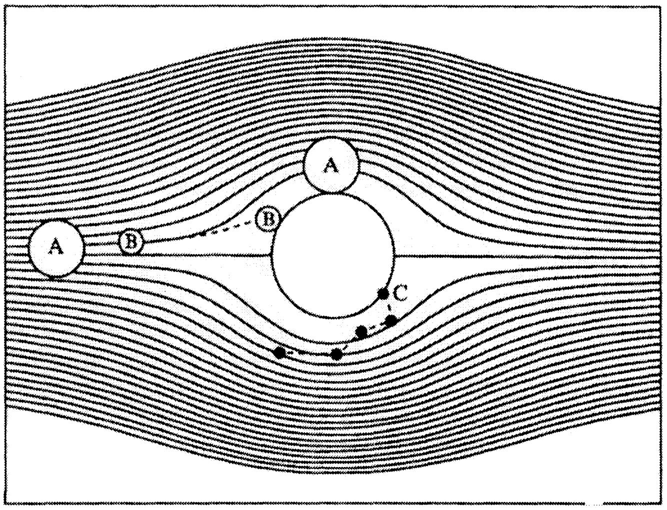

Figure 1. Mechanisms of depostion: A. Interception B. Inertial impaction C. Diffusion [10]

1. Inertial Impaction

As dust laden flow approaches filter media, flow streamlines develop around the individual granules. The high inertia of large particles does not allow them to follow the rapidly changing fluid streamlines, and their trajectories cause them to come in contact with the granule. Collection occurs due to the particle's momentum.

The effects of inertial impaction are usually characterized by the dimensionless Stokes number and apply to particles generally larger than a few microns in diameter [7].

$$St = \frac{\rho_p \cdot d_p^2 \cdot U \cdot C_s}{9 \cdot \mu \cdot d_g}$$

ρ_p = particle density

d_p = particle diameter

U = superficial velocity

C_s = Cunningham factor for molecular slip

μ = gas viscosity

d_g = granule diameter

The superficial velocity is the gas velocity calculated from volumetric flow rate and cross-sectional area of the pipe through which the gas is flowing. Molecular slip is velocity slip at the particle surface. Slip increases as particle size approaches the mean free path length for gas molecules entraining the particle. Inertial impaction is most important for particles greater than 15 μm in diameter, and high superficial gas velocities. Tien declares this mechanism to dominate for Stokes numbers greater than 1.0 [7]. Due to particle size and gas velocity in this research, this mechanism is dominating filtration.

2. Particle Interception

Interception occurs when the gas streamline carrying the dust particle flows near the granule surface. When the dust particle radius is greater than the distance from the granular surface to the streamline, the dust particle makes contact with the granule and is removed from the flow. Interception plays a major role in granular filtrations since there are many possible places for interactions to occur as the flow progresses through the granular bed. This collection mechanism is characterized by the dimensionless Interception number and is defined as the ratio of dust particle diameter to collector granule diameter [11].

$$R = \frac{d_p}{d_g}$$

The high superficial gas velocities force the streamlines to flow near the surface, and a relatively large dust size increases the probability of contact. This is an important mechanism in this research for the large char particles.

3. Particle Diffusion

For particles smaller than 3 μm, collection is governed by random diffusion mechanisms resulting from Brownian motion [7]. As particle size approaches the mean free path distance of the gas molecules, the random diffusion motion of the particle increases. The increase in particle motion increases the probability of particle capture in the filter. The dimensionless Peclet numer is used to characterize diffusion effects, where k is the Boltzman constant and T is the absolute temperature [7].

$$Pe = \frac{3\pi\mu d_p U d_g}{C_s kT}$$

The majority of particles in this research are much larger than 3 μm, and diffusion is not considered in greater detail.

4. Particle Straining

Particle straining occurs when the particulate to be collected is larger in size than the interstitial pores in the granular bed [7]. This mechanism is similar to the sieving of particulate over a uniform grid of desired size holes. Particles that are smaller in size will pass through the grid while larger particles remain behind. No dimensionless number has been defined to characterize this collection mechanism, however dust and granule diameters are important dimensions.

5. Particle Sedimentation

If the particle density is greater than that of gas, then particle will tend to settle out in the direction of the gravitational force. The dimensionless parameter N_g is used to characterize this collection mechanism by relating fluid and particle densities [7].

$$N_g = \frac{d_p^{\,2} g(\rho_p - \rho_f)}{18\mu U}$$

Gravity can be very important for extremely large particles and it can cause large effects when the gas undergoes changes in flow direction [7].

Flagan et al. describe the size ranges for which various mechanisms of collection are important as follows [12]:

Inertial impaction: >1 μm

Interception: >1 μm

Brownian Diffusion: <0.5 μm

All filtration mechanisms are present in the granular filter bed of this research due to the range of particle sizes that exist in the gas flows typical of fast pyrolysis systems, but two mechanisms are dominant in the capture of particles. The majority of the particle sizes are much larger than just a few micrometers, and therefore, inertial impaction and interception are the most important mechanisms when describing granular filtration in this research.

2.2.3 Granular filter applications

Granular filters are being used in a variety of applications in varying designs as noted by Tien [7]: "The significant number of patents granted in recent years to gas-cleaning processes based on granular filtration attest to its enduring utility [7]."

Granular filtration for the purification of water is as old as the Egyptian Empire (200 B.C.) [7]. In modern times, large beds of sand and carbon are used to remove sediments and undesired materials from natural water flows as well as in water and sewage treatment facilities around the world. Applications to gas and air filtration similar to this research have been under development since the early 1900's. Coal combustion and other combustion processes that are used for generation of electricity have been developing granular filtration technology to remove fly ash from the flue gas stream exiting the combustors [13]. The emergence of gasification of biomass in the bio-industry has brought about an investigation into granular filtration technology for a cost effective and reliable hot gas clean-up system for the gas product stream. The National Renewable Energy Lab (NREL) and The Technical Research Center of Finland (VTT) have also begun research in applying granular filtration to pyrolysis to remove the solid char to improve the quality of the condensed pyrolysis liquid [4]. Designing filter systems to optimize filtration mechanisms to reach high efficiencies continues to be a research need for the removal of char in pyrolysis systems.

2.2.4 Types of granular filters

Many different designs of granular filters for gas filtration have been developed for different filtration applications. Granular filters can operate in the fixed bed, moving bed and fluidized bed modes. Fixed bed filtration is inherently non-steady. It is used for high efficiency needs with small particulate loadings that do not require frequent filter cleaning. **Figure 2** displays a typical fixed bed filter arrangement, and physical parameters such as diameter and bed depth may vary.

Clean Gas

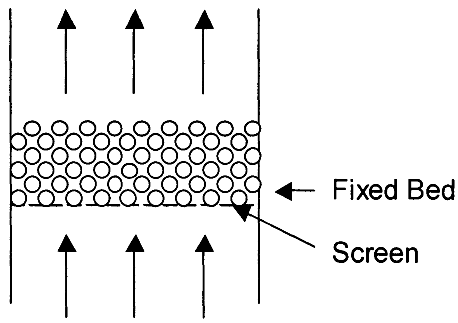

Dirty Gas

Figure 2. Fixed bed granular filter

The static bed allows for deposited material to remain undisturbed in the granular matrix. The increase in deposited material in the granular matrix increases the efficiency of the filter as the interstitial voids decrease in size [14], however the pressure drop continues to increase until a critical value is reached and the filter must be cleaned.

The moving bed filter is operated in a steady state mode where continuous filtration is achieved by replacing dust laden filter media with clean media. The moving nature of the beds disrupts deposited dust, and efficiencies are typically less than static beds under the same conditions [14]. **Figure 3** displays one type of moving bed granular filter where dust-laden gas passes co-currently with the granular bed as dust particles are removed.

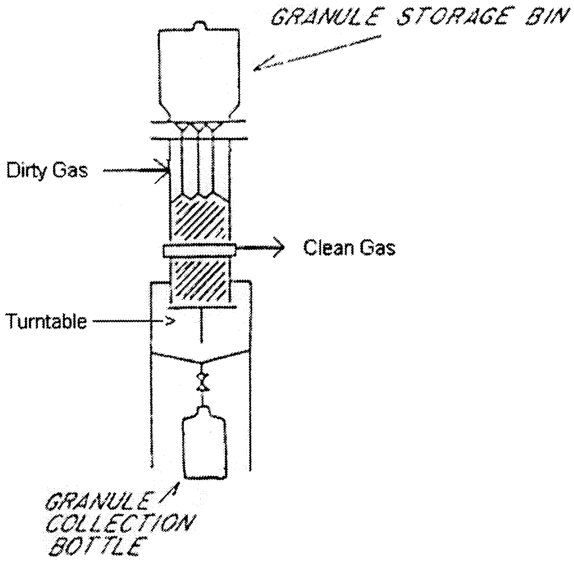

Figure 3. Moving bed granular filter [14]

Fluidized granular filtration operates on the principle of increasing the probability of interaction between dust and the filter granules by increasing the random motion of the filter media in the bed. Typical applications include high velocity gas flows with small dust loadings of sub-micron particulate governed by diffusion and interception mechanisms. Superficial velocity is sufficiently high to overcome the inter-granular and gravitational forces of the granular media. This causes the granular particles of the bed to suspend in the gas flow with random motion and behave more like a fluid. **Figure 4** displays a fluidized granular bed filter arrangement.

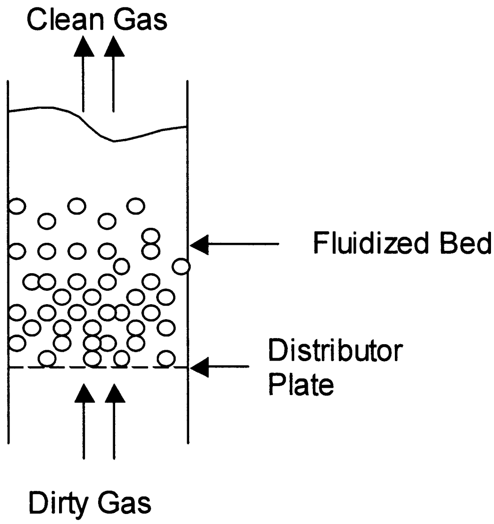

Figure 4. Fluidized bed granular filter

Dusts collected through these mechanisms are less likely to be re-entrained after initial deposition [10]. The adhesion forces for these small particles are large enough that particle collision and drag forces are insufficient to re-entrain collected particles [Brown].

Moving granular bed filters introduce the dust-laden gas to the granular bed with one of three basic methods. Co-current filters introduce the dirty gas in parallel flow with the granular media. For convenience, **Figure 3** is reproduced here as **Figure 5** to display the co-current moving bed granular filter used by Kalinowski et al. [14]. In this arrangement, granules move from the storage bin above the bed through 4 holes in a distributor plate. Dust- laden gas enters above the bed and the clean gas exits from the side of the bed. Granules are retained at the exit by the use of a screen. Granules continue downward until they are dispensed to a collection bottle by a turntable used to control the granular flow rate.

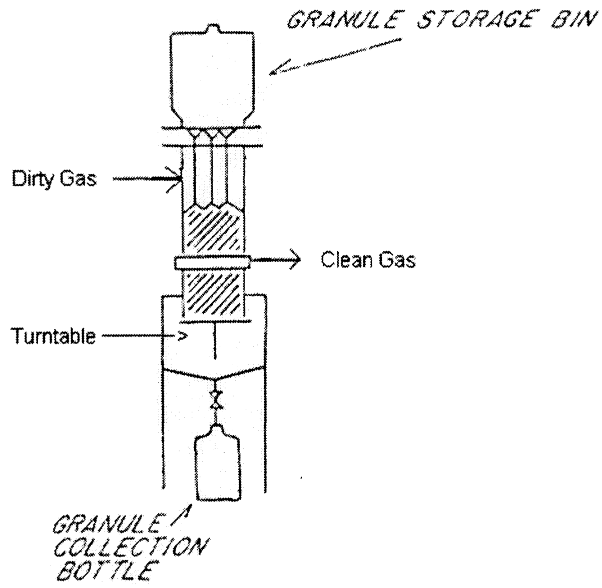

Figure 5. Co-current moving bed granular filter [14]

Gas with the highest dust concentration is introduced to the cleanest of granular media and the clean gas exits from the most dust-laden granular media, which sets a limit on the ultimate efficiency of this design.

Counter-current filters operate so the gas flows against the moving granules. **Figure 6** displays the counter-current flow moving bed granular filter used at Combustion Power Company for high-temperature filtration [15]. This filter injects dust-laden gas into the bottom of the filter, which is cleaned as it passes upward through the downward flow of progressively cleaner granules. Dirty granular media is removed, cleaned and returned to the top of the filter by a re-circulation system. The dust-laden gas is introduced to dirty media and the clean gas exits from the cleanest media.

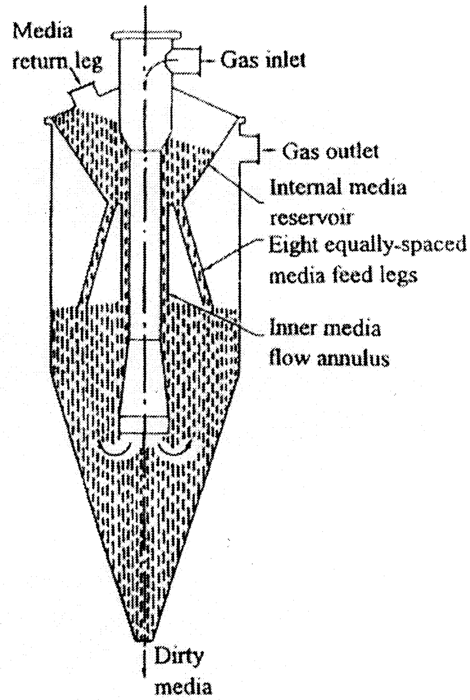

Figure 6. Counter-current moving bed granular filter [15]

The third type is cross-current design where the gas flow is perpendicular to the flow of granular media. Louvered panels or screens hold the moving bed in place as the gas passes through the media for a vertical cross-current filter [16]. **Figure 7** displays the cross-current filter used in experiments by Jordan et al. [16]. The louvered panels retain the granular media and separate the filter into three sections through which different sized granules can be passed. Granular flow rate is controlled with rollers below the granular bed.

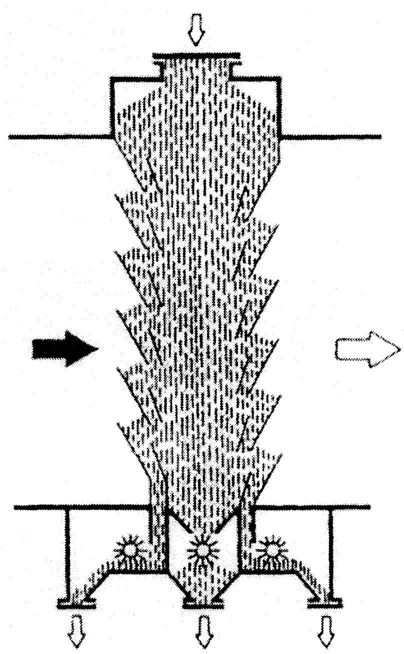

Figure 7. Cross-current moving bed granular filter [16]

These filters require careful designs of louvers to minimize granular movement. Ideal granular flow is plug flow through the filter with no individual granule movement relative to other granules. Another approach to the cross-current filter is the horizontal version used by Tsubaki et al. [17], which carries granules on a conveyor screen through the contaminated gas flow.

The various types of granular filters have multiple designs that try to take advantage of flow properties or particle interactions in an attempt to reach higher efficiencies. Each filter system has advantages and disadvantages, and each application must be evaluated to determine filtration conditions and which design is best suited for the level of filtration desired.

2.2.5 Other parameters in granular filters

Granular flow rate and the size of the granular media are two other important parameters affecting efficiency. Kalinowski et al. concluded that three quarters of the penetrating dust had been previously collected but was re-entrained by collisions due to granular motion [17,18]. Otani et al. concluded that granule velocity has a large impact on filtration efficiency [19]. However, Toyama and Takahashi et al. noted that granules in the center of a pipe flow as if stuck together like a static bed [20,21]. Particle re-entrainment is more likely due to other effects such as particle collisions and increased gas viscosity rather than just granule motion. Soo and Shi concluded that efficiency is more directly related to the ratio of granule to dust flow rates and not just granule flow rate [3, 8].

It is generally believed that a decrease in granule size increases efficiency [9, 22]. Collection efficiency has been correlated to the Stokes number, which is inversely proportional to the granule diameter. This relationship is of the first order and has less of an effect on Stokes number than the second order dependence on changing the dust diameter for the size range used in most applications. Changing the size of the granular media will have more effects on filtration efficiency when the dust to be filtered is of similar size to the granular media. For larger dusts a smaller granule size will lead to more sieving filtration and a higher efficiency as observed by Guillory [23].

Dust properties of size, shape, roughness and Hamaker constants for forces of adhesion are also significant factors affecting efficiency. The size of particles changes their kinetic energy upon collection as well as drag forces exerted on them by the flowing gas. Shape plays an important role in how the particle interacts with the collector surface as well as drag forces. The surface roughness and Hamaker constants based on particle chemical properties change the strength of Van der Waals forces that cause particle adhesion to the collector surface.

The effect of pressure has been found to be small. The viscosity has larger effects on efficiency than density and a change in pressure affects the density and Reynolds number, but the viscosity and Stokes number are relatively independent of the pressure for ranges that are typically experienced in filters. Efficiency tends to decrease for high pressures exceeding a few atmospheres where the viscosity of the gas increases more rapidly [24]. Thus a change in pressure is expected to have little to no effect on efficiency for the pressure ranges of less than one atmosphere experienced in this research.

Temperature also is an important variable to consider in filtration efficiency. Gas viscosity increases with temperature, which increases the ability of the gas to maintain particle suspension and re-entrain captured particles. This may explain why Henriquez et al. concluded that efficiency decreases with increasing temperature [25]. Kuo et al. state that an increase in temperature and pressure increases efficiency only for particles collected by the diffusion mechanism [26,24]. Peukert et al. quantified this by stating that particles smaller than 0.5 μm are collected more efficiently with increasing temperature [27]. Gutfinger et al. confirmed this with experimental data as well [28]. The increase in efficiency is due to increased Brownian diffusion. Peukert et al. also observed improved dust adhesion on the granular surface at higher temperatures [27].

Another attempt to change these particle interaction characteristics is the use of coatings on the granular material. Oil and synthetic coatings have been applied to granules to aid in the capture of particles by reducing bounce and also reduce re-entrainment by increasing the adhesion forces. Periodic or continuous coating of the impaction surfaces can prevent the occurrence of dry spots from which bouncing can occur [29].

The idea of coating the granules leads to another interesting variable that has to do with pyrolysis. It is the effect liquid aerosols present in the influent stream on efficiency. The presence of liquid increases adhesion forces due to surface tension effects and significantly increases filtration [22, 24]. Also, the capillary action between the granule contact points bridges the gaps and increases the surface area available for filtration. When too much liquid is present however, the flow fields around the granules change the characteristics of how the liquid coats the particle surface. Large amounts of liquid increase the distance between the dust particle and the granular surface allowing particulate to move along the granule surface to areas of where drag forces are strongest allowing for increased re-entrainment [30]. The coating on the granule surface also may act to reduce the probability of particle bounce in high gas velocity applications.

Gas velocity is a controversial issue in the literature. The effects of velocity are dependent on dust and granule properties. The inertial filtration of small particles increases with an increase in gas velocity, as confirmed by the experimental results of Knettig et al. [31]. Zevenhoven et al. recorded experimental data that indicated a decrease in efficiency with increasing gas velocity for dust sizes between 0.2 and 2 μm [13]. Larger particles start to experience bouncing effects, which decrease the probability of capture. Large particles that are captured also start to experience larger drag forces that become large enough to re-entrain them in the gas flow. However, extremely small particles dominated by the diffusion filtration are unaffected by changes in gas velocity. The differences in the literature are a result of the wide range of granular filtration media used, different dusts being filtered and the varying designs of filter beds. The importance of gas velocity generally increases as dust particle size increases. In general gas velocities exceeding 1 m/s are considered high, and are generally never tolerated in a high performance filter [24].

3. EXPERIMENTAL METHOD

3.1 Experimental equipment

A schematic of the moving bed granular filter experimental apparatus is shown in **Figure 8**. This moving bed granular filter was designed by Daren Daugaard and Don Stenberg to handle the particulate loading and gas flow rate of the pyrolysis system at the Biomass Energy Conversion Facility (BECON) near Nevada, IA. It is based on designs by Dr. Robert Brown at Iowa State Univeristy to utilizes physical characteristics designed specifically to increase filter performance.

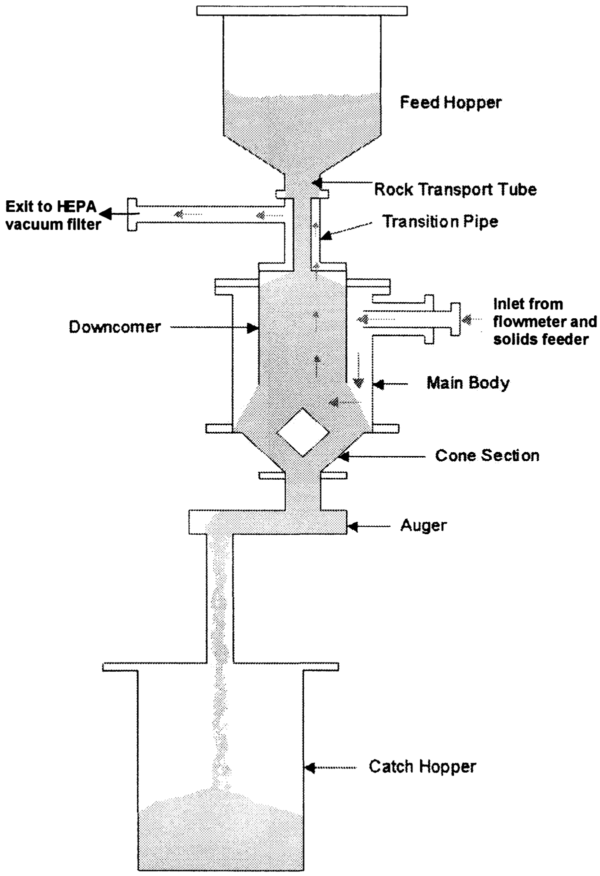

Figure 8. MBGF system schematic [32]

Clean granular media typically 4 mm in size is stored in a feed hopper above the main filter body. Granules flow from the main feed hopper through a 5 cm transport tube to the downcomer section of the main body. The inside diameter of the main filter body is 19.1 cm. The downcomer section is the main granular filtration bed in this arrangement, and bed depth is measured as the depth of granular media inside the downcomer. The typical bed depth is 18 cm. Interchangeable downcomer sections with nominal diameters of 11.4, 12.7 and 15.2 cm have been fabricated for different testing arrangements. **Figure 9** displays some of the important physical dimensions of the MBGF system.

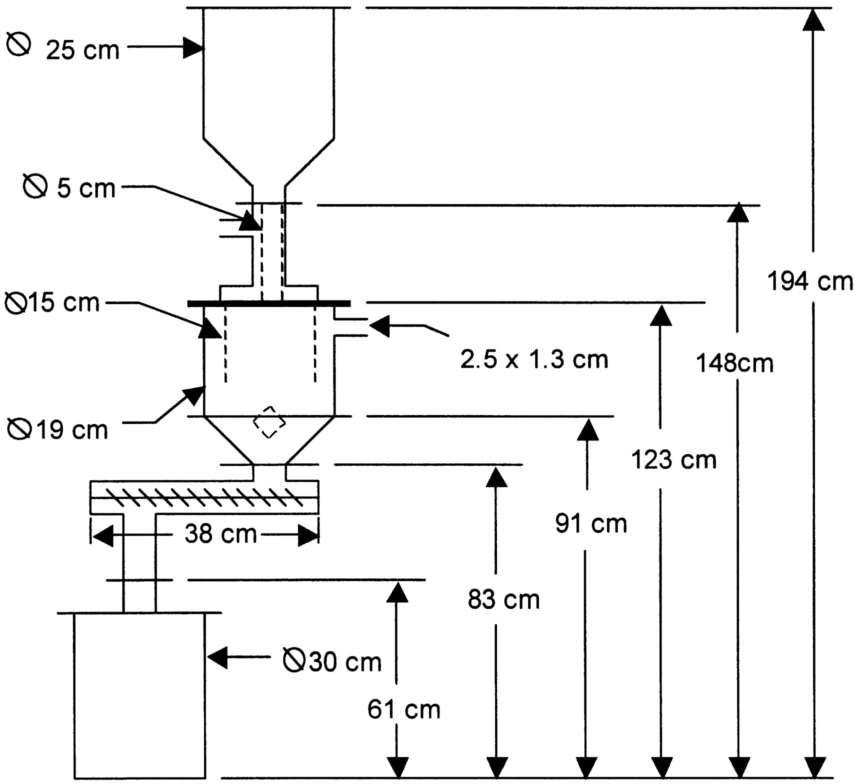

Figure 9. MBGF system dimensions

An auger controlled with a three-phase electric motor and variable frequency drive is located below the main filter body to remove dirty media from the bed. The dirty media is augured into a sealed hopper below the filter.

The square tangential inlet to the filter is designed to induce cyclonic flow at the inlet of the filter to reduce the pressure drop across the filter. The counter-current flow design also incorporates an interfacial region of granular media, which collects high concentrations of dust to increase initial efficiency before entering the main filter bed. This preliminary filtration then allows the gas to flow through progressively cleaner granules and exit from the cleanest granular media near the top of the downcomer. The entire system is designed for simple component interchangeability, which is required to allow for testing of different variables of interest.

The cold flow testing system displayed in **Figure 10**, utilizes compressed air and a Shenck-Accurate model MOD106M bulk solids material feeder to inject a dust-laden air stream to the granular filter. A globe valve is used to control the flow rate, which is measured with a 1-40 scfm Omega variable area flowmeter. See **Appendix B** for the calibration curve. The dust to be filtered is metered into the air stream with the bulk solids feeder. Due to feed rate fluctuations caused by air turbulence and dust bridging in the feeder, an accurate calibration curve was not obtained for the solids feeder. Therefore, the amount of dust injected by the feeder is calculated by measuring the dust in the feeder before and after each individual test.

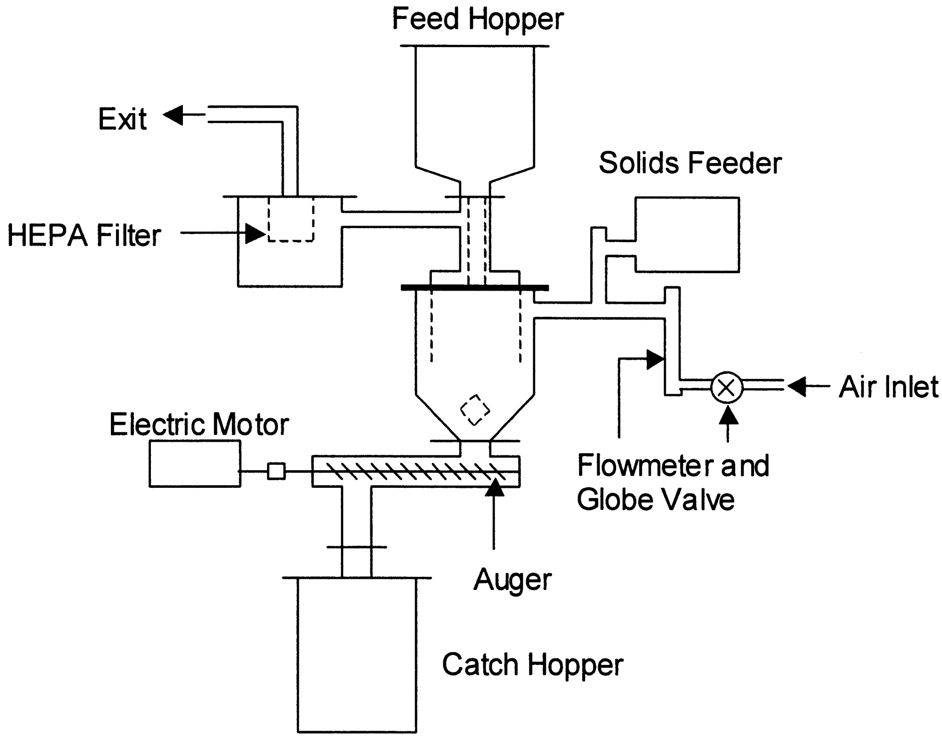

Figure 10. Cold-flow testing system

To measure the dust penetration of the filter, the gas exiting the moving bed filter was passed through a Craftsman Shop-Vac HEPA filter. This filter is stated to be 99.97% efficient at removing dusts down to 0.3 micron. The dusts tested in this research were typically between 5 and 250 micron. The amount of dust injected and dust captured is weighed on a scale with a measuring tolerance of 0.05 grams. An uncertainty analysis for an individual test run is presented in **Appendix C**.

The data acquisition system consists of LabVIEW 5.1 software on a Dell Dimension L500r personal computer that obtains data collected by a National Instruments SCXI-1000 chassis. Through this platform, the signals from several thermocouples and pressure transducers can be collected and recorded. The software records raw data at a desired 1 Hz sample rate and is analyzed in spreadsheet format. Pressure taps are located in positions to measure the gage pressure after the flow meter, the pressure drop across the granular filter and the pressure drop across the Hepa filter. The temperature of the gas flowing through the filter is also monitored with a K-type thermocouple placed at the exit of the MBGF system.

The granular filtration media used was obtained from American Materials Corporation of Eau Claire, Wisconsin. It is defined as Red Flint Gravel and has been cleaned to remove dust and fines. Two media sizes of 4 mm and 2 mm nominally were used and their particle size distributions are presented later in section 3.2 The media is capable of withstanding the high temperature and corrosive environment of the pyrolysis system.

Nunez tested the effects of similar granular material escaping a granular bed filter system with a gas velocity of 1.5 m/s by conducting a material analysis on the effluent stream [33]. No traces of filter media were found to be exiting the filter [33]. Superficial gas velocities of this research are less than 1.5 m/s so no filter media should be exiting the filter bed.

Fluidization tests for both granular sizes were conducted prior to testing filtration efficiency to ensure fluidization did not occur. To determine the fluidization velocity for a given particle size, a clear pipe with a known diameter was partially filled with granules. The gas flow rate through the granules was slowly increased until the granules began to move. The flow rate was noted just before granule movement, and the fluidization velocity calculated using the pipe area and the gas flow rate. See **Appendix E** for fluidization velocity calculation. The fluidization velocities of the granules in this research are less 1.5 m/s, and gas velocities in the downcomer during this research did not exceed the fluidization velocity of the granular media. Thus granular media in the effluent should not be present to affect filtration efficiency. The chemical composition is a follows [33]:

Table 1. Filter media chemical composition

Chemical Compound	% Composition
Silica (SiO_2)	92.87
Iron Oxide (Fe_2O_3)	3.42
Loss on Ignition (L.O.I.)	1.15
Aluminum Oxide (Al_2O_3)	1.25
Magnesium Oxide (MgO)	0.60
Calcium Oxide (CaO)	0.51
Titanium Oxide(TiO_2)	0.04
Sodium Oxide (Na_2O)	0.05
Potassium Oxide (K_2O)	0.06
Sulfur Trioxide (SO_3)	0.04
Barium Oxide (BaO)	0.01

3.2 Particle size distribution

A Ro-Tap CE Tyler B mechanical sieving machine and the ATM Co. LP3 sonic sifter were utilized to obtain particle size distributions to determine an average particle size for the dusts and granular media to be used. To determine the average particle size, a sample of the particles is placed into the top sieve. The equipment is allowed to sift for a short period of time to allow the different particle sizes to separate and be collected in different sized sieves in the stack. The collection of particles in each sieve is then weighed and the sieve size noted. Mathematical formulas from Herdan are then used to calculate the average particle size [34].

The particle size distributions for fly ash, oak pyrolysis char and two different sizes of granular media are presented in **Figures 11-14**. The average particle size for the coal-derived fly ash is 14 μm. The distribution is concentrated around the two nominal sizes of 8 and 85 μm.

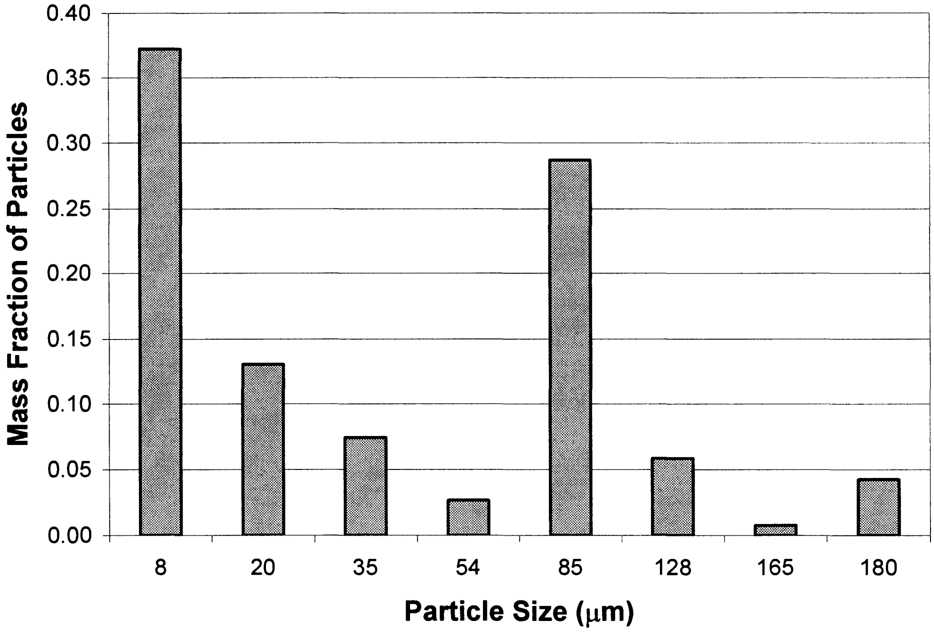

Figure 11. Coal-derived fly ash particle size distribution

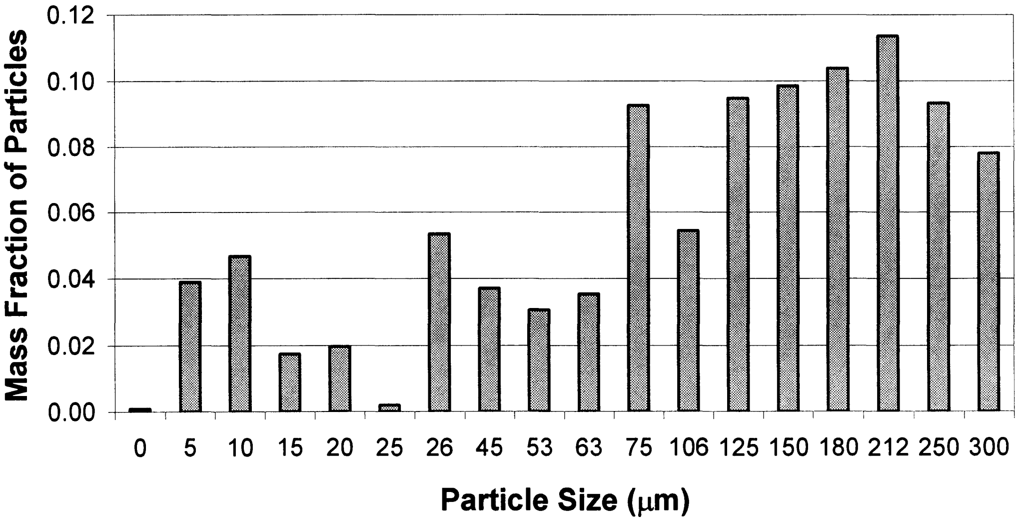

Figure 12. Oak pyrolysis char particle size distribution

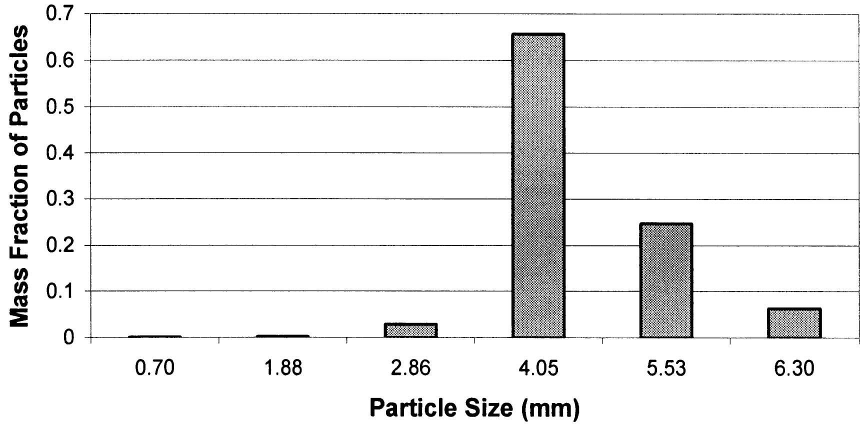

Figure 13. 4mm granule size distribution

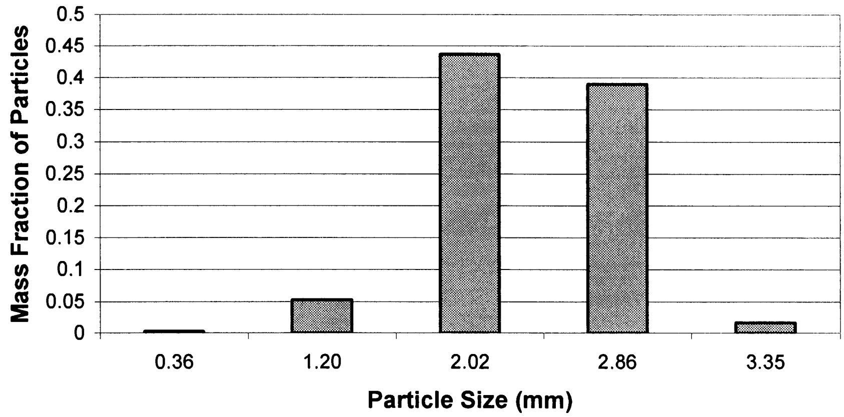

Figure 14. 2mm granule size distribution

The particle size distribution of oak char is more disperse than the coal derived fly ash. The average particle size of the oak char is 52 μm, and a large fraction of the particles are larger than 100 μm. The fly ash does not have many particles with sizes over 100 μm. The size distributions of the granular material are tightly concentrated with average particle sizes of 4.3 mm and 2.4 mm.

3.3 Experimental method

The dust to be tested is first weighed before being loaded into the solids feeder. The feeder lid is sealed and secured to the feeder hopper using two fabricated screw down type clamps. The injection auger from the feeder is inserted into the injection pipe system and sealed with a rubber hose and hose clamps. The HEPA filter is then weighed on the scale before it is sealed and fastened into place on the lid of the filter box. The weight of the filter and dust in the solids feeder is recorded. The lid for the filter box is then sealed, and the box is attached to the moving bed granular filter and the exit pipe with standard pipe couplers.

The granular media is sifted to remove fine particulate before the MBGF system is filled and sealed. The data acquisition system is activated, and the desired granule flow rate is set and activated using a Toshiba Tosvert VFS7-4007UPL variable frequency drive. The calibration curve for the granule flow rate is presented in **Appendix D**.

The airflow is then turned on and the flow is increased to the desired flow rate. The gas flow rate for the system is set at 21 cfm which would be a typical gas velocity if the filter was used with the fast pyrolysis system at BECON (see **Appendix B**). The data acquisition system is then set to record data and the solids feeder is set for the desired feed rate and started. Throughout the test, periodic tapping on the solids feeder to break up bridged dust is necessary to obtain even solids flow.

To terminate a test, the solids feeder and data recording systems are turned off. The air is then shut down followed by the granular control auger. The pressure hoses are disconnected, and the HEPA filter system is removed. The HEPA filter is then removed and weighed with the rest of the dust that has collected on the walls and in the bottom of the filter box.

The dust in the solids feeder is weighed. The weight data is recorded and entered into an efficiency and uncertainty calculation spreadsheet. See **Appendix A** for a sample calculation of efficiency. Finally the dirty media is emptied from the MBGF system. The HEPA filter surface is cleaned with a vacuum cleaner to remove the bulk of the dust.

3.4 Modeling method

It is useful to engineers to have a correlation describing filtration efficiency based on parameters that are easily known before the design process begins. The filtration of dust from a gas stream is similar to the chemical adsorption process of a chemical species contained in a gas flow to the catalyst surface. Parameters of catalyst bed height, gas velocity and concentration of chemical species used in this correlation are similar to granular bed height, gas velocity and fly ash concentration. A derivation from the mass balance equation presented by Wheeler for chemical adsorption processes will be investigated to describe the filtration process [35].

Mass balance on a moving bed filter:

$$\frac{\partial C}{\partial t} + U\frac{\partial C}{\partial x} = R(C,W)$$

R is the rate of removal of fly ash from the gas stream, U is the superficial gas velocity through the bed, C is the gas-phase concentration of dust, W is weight of fly ash retained in the filter bed, t is time and x is the distance into the bed. A first-order rate expression for the removal of fly ash is assumed:

$$R = -kC\ .$$

The value of k is assumed to be a constant, which defines the rate of removal of fly ash for a defined concentration. For steady-state fly ash concentration and gas flow, mass balance simplifies to:

$$U\frac{\partial C}{\partial x} = -kC$$

Integrating this expression over the height of the bed (L), where the fly ash concentration entering the filter is Co, yields:

$$C/C_0 = \exp\ (\text{-k}\ L/U)$$

Recognizing that filter efficiency is defined by:

$$\eta = 1\text{-}C/C_0$$

Filter efficiency becomes:

$$\eta = 1\text{-}\exp\ (\text{-k}\ L/U)$$

Thus it has been determined from this derivation that a parameter defined as the ratio of the downcomer bed height (L) to the superficial velocity (U) in the bed should correlate with penetration. Penetration (P) is the defined with respect to efficiency (η) as follows:

$$P = 1\text{-}\eta$$

The final form of the equation thus becomes:

$$P = \exp\ (\text{-k}\ L/U)$$

Brown and Amundson have also developed similar relations for processes involving the removal of species from a flowing liquid in beds of solid material [10,36].

The literature also includes various other relations similar that could potentially apply to granular filtration. These other equations are dependent on the single granule collection efficiency derived using other models [37]. This approach is dependent on theoretical models for gas flow through the granular bed, and is not convenient for design engineers. The developed model is based on bed height and superficial velocity, which are much more convenient for design engineers to work with.

It should be noted that k has been assumed to be a constant in this development. In terms of granular bed filtration, k is a layer efficiency of the bed. The Stokes number governs the efficiency of filter beds operated in the inertial impaction collection regime. Thus, k may have a dependence on gas velocity and density, particle size and granule size. The constant assumption is based on the small range of gas velocities used and with all other parameters are held constant.

4. EXPERIMENTAL RESULTS AND DISCUSSION

4.1 Experiment design

Experiments were designed to identify which physical parameters of the MBGF system are most important to high efficiency operation of the moving bed granular filter. Parameters such as downcomer diameter, interfacial area, filter bed height, superficial velocity, granule size and the presence of flow straightening fins were investigated. Fly ash was chosen as the dust for cold flow testing for its availability and ease of handling. It was also desired to determine if high removal efficiency for pyrolysis char is obtainable under similar cold flow testing conditions as the fly ash.

4.2 Comparing effects of interfacial area to downcomer area on efficiency

In previous work with a similar system, the conclusion was drawn that high filtration efficiencies were partially due to dust buildup in the interfacial region of the system (See **Figure 15**) [3]. **Figure 15** is presented to identify area discussed within the body of the moving bed granular filter of this research. The interfacial region is the area where the dust-laden gas first encounters the cascading granular media from the central downcomer. The downcomer is considered the bed of granular material flowing on the inside of the filter. The figure also displays the tangential inlet to the filter and the resulting cyclonic gas flow. It also shows the presence of flow straightening fins and arrows to indicate the direction of gas flow through the filter.

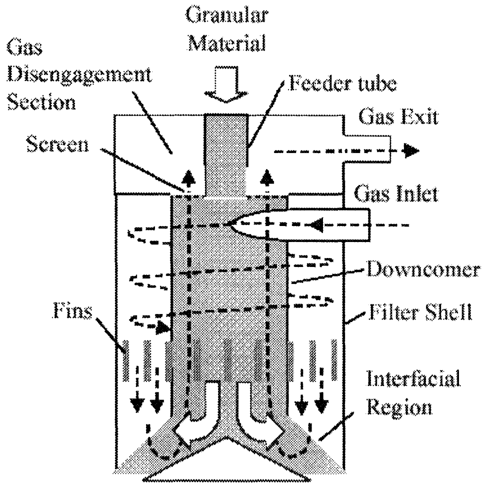

Figure 15. Sections in MBGF system [8]

Results and discussion of Soo focused on the interfacial area and the effects of the actual downcomer bed diameter were not discussed [3].

These experiments were designed to maintain a constant downcomer area inside while varying the outside interfacial area by using inserts in the downcomer section. All other variables were maintained constant. The fins that had been designed for the system were not used in these testing arrangements to eliminate confounding effects on tests.

If the interfacial region is affecting the overall efficiency of the system, then increasing the gas velocity in the interfacial region should decrease the removal efficiency. Three tests were conducted under each of the two downcomer arrangements. The results in **Table 2** display the averages and their corresponding 95% confidence intervals.

The results show that changing the interfacial area has an effect on the overall efficiency when the downcomer area is held constant. There is convincing statistical evidence to verify there is a difference between the two system arrangements.

Table 2. Effect of changing interfacial area on efficiency

Downcomer Area **Downcomer Velocity**	$0.010\ m^2$ 1.2 m/s	
Interfacial Area	**Interfacial Velocity**	**Efficiency**
$0.016\ m^2$	0.626 m/s	96.23 ± 1.75 %
$0.006\ m^2$	1.58 m/s	85.88 ± 9.29 %

Using the t-statistic method for determining if a difference exists between two means yielded a two-sided p-value less than 0.01. Since velocity in the downcomer was held constant for these tests, this analysis verifies that the area of the interfacial region is affecting the overall efficiency of the system.

The next tests were designed to investigate the importance of downcomer area on overall efficiency. The interfacial area of the filter was held constant, and downcomer inserts were used to vary the downcomer area. If the downcomer area is important to the overall efficiency of the system, then increasing the superficial velocity in the downcomer by decreasing the downcomer area should decrease efficiency. The results in **Table 3** display the averages and 95% confidence intervals.

Comparison of the data demonstrates that decreasing the downcomer area causes a decrease in the overall efficiency of the filter system. A t-test of a statistical difference between the two arrangements yields a two-sided p-value less than 0.01.

Table 3. Effect of changing downcomer area on efficiency

Interfacial Area	0.006 m^2	
Interfacial Velocity	1.58 m/s	
Downcomer Area	**Downcomer Velocity**	**Efficiency**
0.019 m^2	0.532 m/s	97.32 ± 0.31 %
0.010 m^2	1.2 m/s	85.88 ± 9.29 %

This confirms that the area of the downcomer section has an important affect on the overall efficiency of the filter system.

The results of testing these two filter parameters indicate that the design of a highly efficient filter may include relatively high filtration velocities in the interfacial region if the downcomer velocity is kept relatively slow. A gas velocity of 1 m/s is considered a high velocity in conventional barrier filters [24]. Even when the interfacial velocity exceeds 1 m/s, high efficiencies can be achieved if the downcomer velocity is slow, as seen in **Table 3**. This agrees with the conclusion drawn by Brown et al. [38]. High interfacial velocities force high inertia particles toward the outside of the filter body due to the cyclonic action imparted to the gas flow by the tangential inlet to the filter depicted in **Figure 15**. The granule movement removes the dust particles near the outside of the filter body as the gas progresses up the downcomer section of the bed. Therefore the downcomer can be designed to take advantage of cyclonic filtration prior to the gas entering the granular bed.

The results also show that superficial velocities in the downcomer could be relatively high compared to 1 m/s as long as the minimum fluidization velocity of the granular material is not exceeded. High superficial velocities in the downcomer also requires that the velocity of the gas in the interfacial region remain slow to achieve high levels of efficiency as depicted in **Table 2**.

4.3 Experiment of flow straightening fins

The high efficiency conclusion about the interfacial region drawn by Soo and Wistrom also led to the inclusion of flat plates called fins, which are mounted on the outside of the downcomer and extend from the downcomer surface to the inner surface of the filter body [3,39]. The purpose of the fins is to force the gas flow downward through the interfacial region to avoid granule and deposited dust layer disruption. Cyclonic flow of high velocity interfacial gas was believed to cause dust re-entrainment by agitating the granule-gas interface and the layer of dust deposited on it [39]. If this conclusion were true, then the removal of the flow straightening fins of this MBGF system should cause a decrease in efficiency when compared to tests with fins in place.

To test this hypothesis, all three different diameter downcomer sections were tested with a series of three tests for each diameter. Then the fins were removed from all three of the downcomer sections used in the system to conduct another series of three tests with each. All other variables were maintained constant. The no-fin results are compared with tests that have fins in place in **Table 4**. Numbers presented are averages with 95% confidence interval tolerances. See **Appendix D** for an example calculation.

Table 4. Summary of fin testing results

Nominal Downcomer Size	Fins Present	No Fins	Test Difference P-Value	Statistical Conclusion
11.4 cm	96.43 ± 1.62 %	96.23 ± 1.75 %	>0.25	No Difference
12.7 cm	97.23 ± 2.60 %	98.22 ± 0.88 %	>0.05	No Difference
15.2 cm	96.58 ± 3.01 %	97.32 ± 0.31 %	>0.15	No Difference

Comparing the averages from the different test arrangements, the presence of fins decreases the overall efficiency of the MBGF system for the 15.2 cm and 12.7 cm nominal downcomer sizes. The 11.4 cm nominal downcomer size had similar efficiencies with and without flow straightening fines. Large random variation of efficiencies for a given system arrangement do not allow the conclusion of a statistical difference between the no-fin and fin-included test arrangement results, which led to the decision to not have fins present for subsequent testing.

4.4 Experiment of granular media size

The design of the experiments to test granular size on the MBGF system in this research utilizes the largest diameter downcomer section to maintain superficial gas velocities below fluidization levels. A series of three test trials was conducted for each of the two granule sizes while all other variables were held constant. The averages of the three test trials with 95% confidence intervals are displayed in **Table 5**.

Table 5. Efficiency comparison of 4mm vs. 2mm granular media

Granule Size	Average Efficiency
4 mm	95.86 ± 2.10 %
2 mm	96.95 ± 2.24 %

The data indicate that the smaller rock has a slightly higher average efficiency than the larger rock, however the large random variation between tests does not provide convincing evidence for the conclusion of a difference based on statistical analysis.

Using smaller rock for the filtration of pyrolysis char made achieving steady-state filtration more difficult. The granule flow rate had to be increased periodically as the pressure drop across the filter often increased rapidly as dust was deposited in the filter. Overall efficiencies of the smaller granule tests did increase compared to the larger granule tests, but direct comparisons are not valid due to the increase in granule flow rates. A second test on the smaller rock with a higher granule flow rate was able to reach steady state operation. A summary of the pyrolysis char test results appears in **Table 6**.

Efficiencies in the filtration of char and fly ash increased with the reduction in granule size. The decrease in granule size had a larger effect on the filtration of char than for fly ash.

Table 6. Summary of pyrolysis char test results

	4mm Granules	2mm Granules	2mm Granules
Granule Flow Rate	4.1 kg/hr	Variable	18.4 kg/hr
Efficiency	67.46%	82.94%	71.84%

A possible reason for this is the relative size of each dust particle compared to the granules. Char has more particles larger than 100 mm where fly ash does not. As the granule size is decreased, the sizes of the interstitial voids are decreased as well. This decrease in void size would contribute to more sieving filtration of large particles, where small particles would remain relatively unaffected by the change in void size.

4.5 Experiment of the ratio of bed height to superficial velocity

The experiments to test the new correlation between penetration and L/U developed in section 3.4 were designed to obtain values of penetration for a broad range of values for L/U. To change the downcomer bed height (L), different length transport pipes were constructed that transfer granules from the hopper to the downcomer. As the longer transport pipes are inserted, the height of the downcomer bed decreases. **Figure 16** displays the relationship between transport pipes and bed heights. A series of 6 different length transport pipes were utilized. An extension section of 61.9 cm was constructed to increase the initial bed height from 18 cm inches to 79.7 cm. The different combinations that were assembled with these interchangeable parts allowed a bed height range of 5 to

79.7 cm to be tested. The superficial velocity (*U*) is varied by increasing or decreasing the volumetric flow rate. **Appendix F** presents calculations of the superficial velocity.

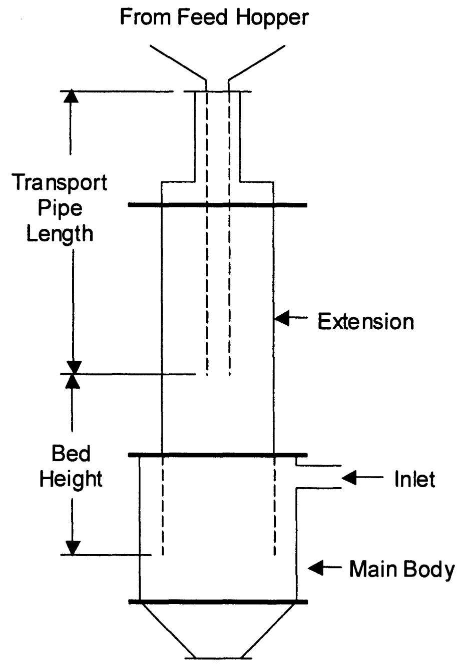

Figure 16. Transport pipe relationship to bed height

Flow rates of 15 (triangles), 20 (diamonds) and 25 cfm (squares) were used for each of the system arrangements. The data results from the series of tests conducted are presented in **Figure 17**. **Figure 17** is a descriptive tool in analyzing what is happening in the MBGF system as well as knowing how changing bed height and superficial velocity will affect the performance of the filter. It should be noted that if the filter bed height were to be zero, theory would expect that all of the dust would penetrate the filter yielding a value of 1. This plot does not go through the unity point due to filtration effects of the cyclonic action in the filter and the presence of a granular interface between the bed and the dust-laden air stream.

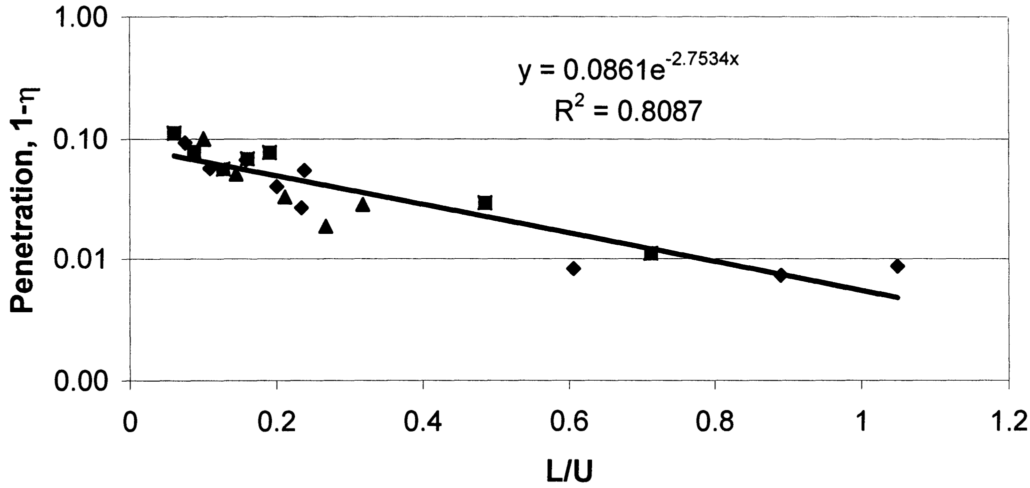

Figure 17. Semi-log plot of experimental data

From the intercept of the linear regression line it can be determined that the efficiency due to these effects is 91%. The surface filtration phenomena was also noted by Thambimuthu et al. and used in their formulation of a very similar equation describing filter efficiency for a static granular bed [40].

$$C = (1-\delta_0)C_0 \exp(\frac{-K_M m}{AU})$$

C is the concentration at a given bed mass m. C_o is initial concentration entering the bed. K_M is the collection rate constant per unit bed mass. A is the cross-sectional area and U is the superficial velocity. The term (1-δ_0) is the correction factor for the surface filtration phenomena.

Thus Soo and Shi's conclusions of relatively high efficiencies at the interfacial region of the MBGF system are in agreement with this research [3] [8]. It is still not well understood if the cyclonic action is responsible for the high interfacial efficiency or if it is the development of a dust cake at the interface. The build-up of a dust layer on the surface of the granular media in this research has not been observed when disassembling the filter. The filter was not disassembled after every trial. The surface of the granules had a light coating of fly ash similar to the granules on the inside of the downcomer in tests where the filter was disassembled. These observations were after tests with high as well as low interfacial velocities. Other researchers have visually observed the dust layer formation in their research and attribute high levels of interfacial efficiency due to this layer [8] [39] [41]. The lack of this visual evidence is leading to the conclusion that cyclonic action is causing high levels of interfacial efficiency.

R.C. Brown noted that aerosols with disperse size distributions cause inflection points in these plots due to different particle sizes having different filtration efficiencies [10]. The overall efficiency of the filter is the sum of the individual efficiencies for the different particles sizes in the dust distribution: "The least penetrating particles are captured early in the passage of the aerosol through the filter, with the result that the remaining aerosol is relatively depleted of easily captured particles and is therefore more penetrating [10]." The result is an upward concavity in the plot.

The number of dust particles collected in a filter bed is proportional to the number of dust particles entering the bed, depth of the bed and a constant describing the efficiency. This constant is termed the layer efficiency α. When the log of particles penetrating the bed is plotted verses the bed thickness, the slope of the resulting line is equivalent to the layer efficiency. A poly-disperse dust of two particle sizes will have an upward concave plot with layer efficiencies equal to the slopes of the lines before and after the inflexion point. Removal efficiencies of various particle sizes are needed to determine which sizes have the higher layer efficiencies.

Particle size distributions of fly ash before and after being filtered by the MBGF system were created and compared to calculate single particle efficiencies for the various sized particles of fly ash. **Figure 18** presents the particle size efficiencies for fly ash. From the graph it can be concluded that the small and large particles have the higher filtration efficiencies than medium sized particles.

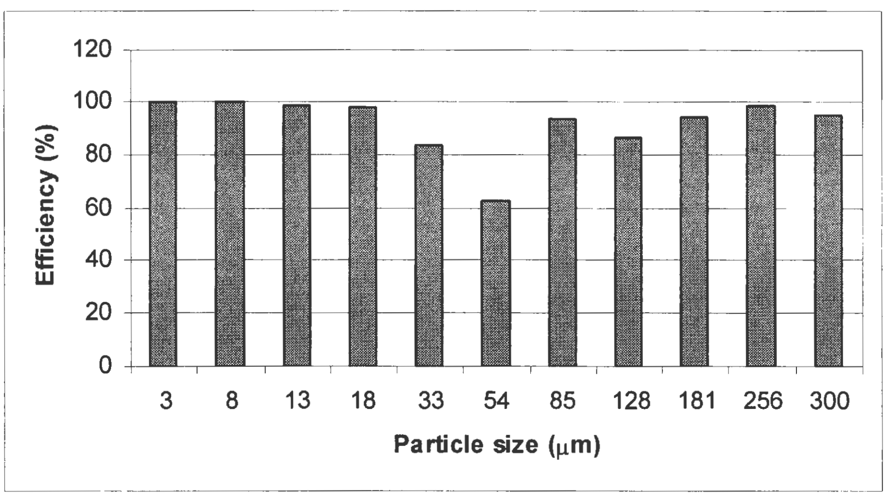

Figure 18. Single particle efficiencies for fly ash

The negative efficiencies represent particle sizes where the mass fractions of those particles increased through filtration of the small and large particles while leaving behind the medium sized particles. Thus small and larger fly ash particles have high layer efficiencies. It can be seen from **Figure 18** that different sized particles have very different filtration efficiencies based on the effects of the five main filtration mechanisms. The poly-disperse model suggested by Brown is thus more appropriate in describing the filtration characteristics [10].

A poly-disperse model was fit to the fly ash data using MathCad assuming two particle sizes of 8 and 85 μm based on the particle size distribution displayed in **Figure 11** of section 3.2. The model for penetration, P, takes the following form [10]:

$$P = (1 - f)\exp(-\alpha_1 L / U) + f \exp(-\alpha_2 L / U)$$

f is the mass fraction of one particle size and the α's are proportional to the layer efficiency. Each size range was assumed to consist of 50% of the material so f and $1-f$ are both 0.5. The experimental data is compared to this bi-modal model based on the full data set and the mono-disperse model based on the first ten data points in **Figure 19**.

The bi-modal model appears to be a better match to the experimental data than the mono-disperse model. The disperse particle size of fly ash is affecting the values of penetration for a given L/U. MathCad yielded values of 9.904 and 2.044 for α_1 and α_2. It is clear from the α values that the two particle sizes considered have very different layer efficiencies, but the model does not define which sized particles have the higher efficiency.

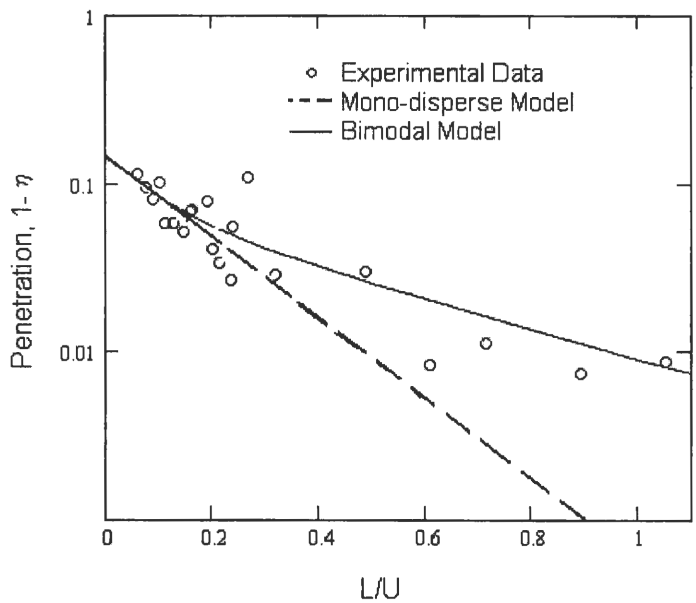

Figure 19. Poly-disperse dust filtration model

4.6 Application to filtration of pyrolysis char

The cold flow testing discussed up to this point has been with coal-derived fly ash, which has particles smaller and more dense than typical of char generated during fast pyrolysis of fly ash. Recognizing that these differences in particle properties could result in dramatic differences in Stokes number and thus filtration efficiency, a series of experiments were performed with gas flows containing char particles instead of fly ash.

The testing procedures for the char particles duplicate that for fly ash. However, char has bulk density of 400 kg/m^3 compared to 1260 kg/m^3 for fly ash so the dust injection rates from the solids feeder are much different on a mass basis. Fly ash is typically injected at 1 kg per hour nominal feed rate while char can only be fed at a rate of 0.4 kg per hour.

Two tests were done to compare changing *L/U* values similar to the experiments for fly ash described in section 4.5. The first test used 18.1 cm for the value of *L*, and the second test used 79.7 cm. The shallower bed yielded a filtration efficiency of 67.46% while the deeper bed only yielded 64.35% efficiency. The tests indicate that the filtration efficiency of char is much less than fly ash and there was no evidence of dependence on bed height or superficial velocity.

Visual images from an electron microscope are shown in **Figures 20** and **21. Figure 20** is a picture of a char sample from the char that is used to inject into the MBGF system. **Figure 21** is picture of a sample taken from the char that penetrates the MBGF system. The presence of fine char particles causes the picture of the char before filtration appear blurred and soft, where as the picture of the penetrating char is vivid and clear. It should also be noted the fibrous shape of the char particles and the large surface irregularities present.

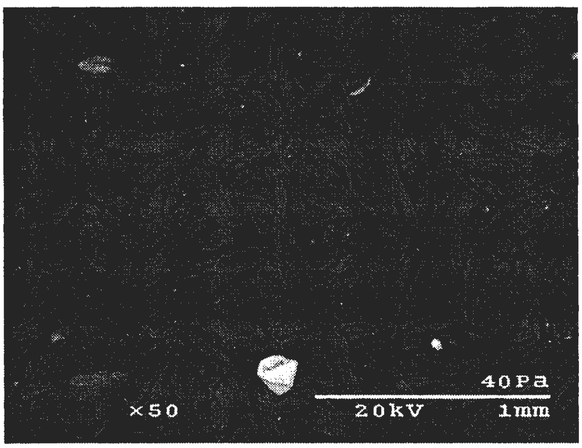

Figure 20. Oak char before MBGF filtration

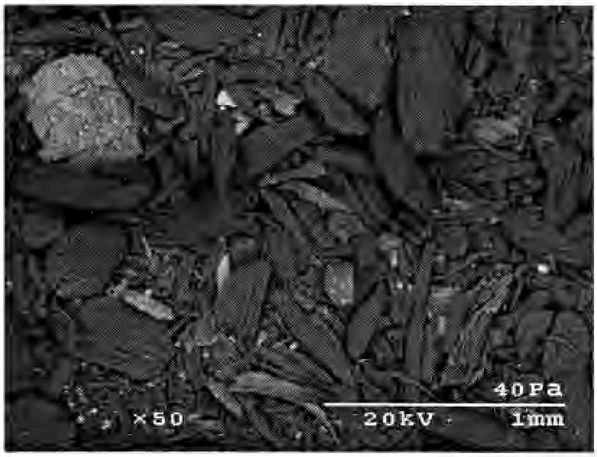

Figure 21. Oak char after MBGF filtration

The distribution of different char particle size filtration efficiencies is shown in **Figure 22**. A comparison of the average particle size for the two char samples reveals a shift to larger particle sizes. The average particle size increased from 52 μm for initial char to 186 μm for char that has penetrated the MBGF system. The MBGF system is removing the smaller particles more efficiently while large char particles are penetrating the filter bed.

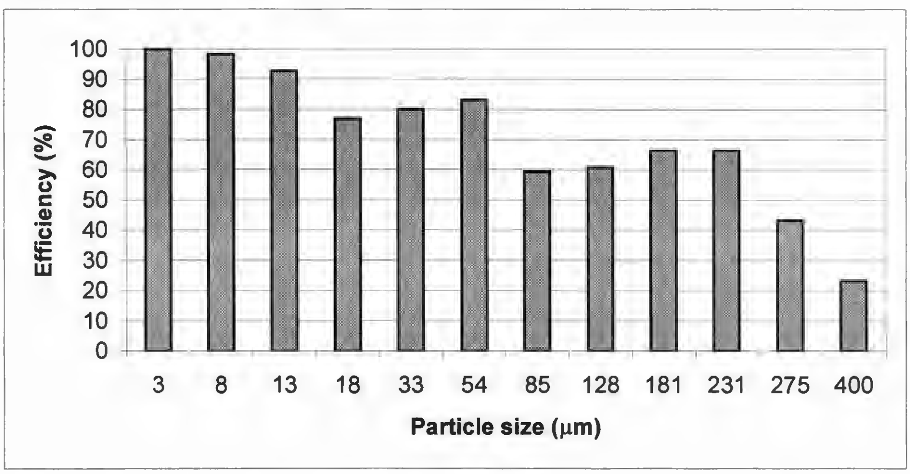

Figure 22. Particle size efficiencies for char

The graph indicates that the MBGF system has efficiencies less than 90% for the removal of char particles larger than 8 μm.

Reduction in granule size did show some improvement on char filtration efficiency. Four millimeter diameter granular media removed char with 67.46% efficiency while the smaller 2 mm granular media removed char at 71.84% efficiency as noted in **Table 5** of section 4.4. This improvement was due to the reduction in size of the interstitial voids within the granular media. The overall voidage volume for both granule sizes is about 40%, but the smaller granules present smaller flow areas between the granules, which increases the probability that large, high kinetic energy particles will be removed by straining.

One explanation of the reduced efficiency for char is the effect of increasing Stokes number on particle bounce. Generally, an increasing Stokes number increases the particle impaction and interception filtration efficiencies by causing gas stream lines to flow closer to the granule surface and change more abruptly as they approach the granules. Kuo et al. states that collection efficiency of granular beds is larger than 90% for Stokes Numbers greater than 0.01 [26]. It is more likely that the probability of dust particles coming into contact with the filtration surface is greater than 90%, but this efficiency does not describe the actual particle collection. When Stokes number reaches a critical size, the particles have enough kinetic energy to rebound from the granule surface. Particles that do not rebound from the surface are unlikely to be re-entrained [10].

Particle rebound from the granule surface is defined as particle bounce, and the particles are not collected. R.C. Brown, Yoshida and Chi Tien claim that onset significant particle bounce occurs at a Stokes number of 0.01, and they each define a particle adhesion probability based on this crucial dimensionless number [10][42][7]. **Table** 7 below lists some of the various Stokes numbers associated with the fly ash and char in this research. The numbers are based on the average geometrical particle size determined from the particle size distribution.

Table 7. Stokes numbers

	Interfacial Region	Downcomer Region
	St	St
Fly ash	0.98	0.42
Char	1.81	0.78

The Stokes numbers for this research significantly exceed the 0.01 standard for bounce. The fly ash has lower Stokes numbers than the char, which is a probable reason why the fly ash filters with much higher efficiencies than the char. Tardos et al. also explained deviations from the predicted model during testing to be the result of increasing kinetic energy and the indication of particle bounce [37]. The fly ash achieves very high efficiencies even though the 0.01 value is exceeded. This suggests that other properties of the dust and the granular media must have an effect on filtration efficiencies. Tardos et al. declare that efficiency must be a function of Reynolds number and Stokes number [37]. They define this relationship with a modified Stokes number based on Reynolds number as the proper variable that combines these two parameters. The Reynolds number correction corrects for the difference between geometric diameter and hydraulic diameter. The hydraulic diameter better expresses the drag forces a fluid applies to the particle. It is expressed as follows:

$$St' = St*(1+0.0157*Re)$$

Table 8 compares this modified Stokes numbers for fly ash and pyrolysis char based on average particle size. The difference between numbers for fly ash and char are nearly a factor of two and provide a more significant explanation for the large decrease in filtration efficiency of pyrolysis char. Higher values of St' indicate higher kinetic energy of dust particles mainly due to larger particle size and an increase in drag forces on the particles by flowing gas. Wang et al. also found particle bounce to be a strong function of particle size [43]. Deviations of experimental results from predicted filtration efficiencies should be more significant with higher particulate kinetic energy [37].

Table 8. Modified Stokes numbers

	Interfacial Region	Downcomer Region
	St'	St'
Fly ash	5.92	1.33
Char	10.97	2.46

The high values of Stokes and Modified Stokes numbers indicate that significant bounce is likely to occur for pyrolysis char. As char particles impact and rebound from the surface of the granular media, they proceed to the next layer of granules with less kinetic energy than the previous impaction. Subsequent impacts continue to reduce the amount of kinetic energy of the char particles. After a sufficient number of impactions, the char particles should lose a significant amount of kinetic energy and finally be collected deep in the bed. Filtration of char with a deeper bed did not indicate an increase in efficiency. Other properties are thus likely to be causing poor efficiency.

R. C. Brown states the presence of a wide range of other important dust and collector properties in his book [10]. The properties of the dust particles are the most dominant in affecting removal efficiencies. Properties of shape, density, hardness, surface roughness and particle size are important, although it is very difficult to isolate a single effect in experiments [10].

Table 9 compares five dusts with varying properties used to identify these important characteristics. They are arranged from left to right in the order of increasing filtration efficiency. Particle sizes are very similar and the main differences are density, particle shape and surface roughness.

Table 9. Properties of different test dusts [44]

	Fly ash	Calcium carbonate	Cornstarch	Pine	Oak Char
Size (μm)	14	10	10	15	13
Density (kg/m^3)	2600	2700	1500	430	560
Filtration Efficiency (%)	97.32	94.67	91.15	82.49	66.20

The shape is an important property that affects how the particle responds to the hydrodynamic gas flow that is suspending the particle. Comparing the shape of fly ash in **Figure 23** to the shape of calcium carbonate in **Figure 24**, the fly ash is much more spherical.

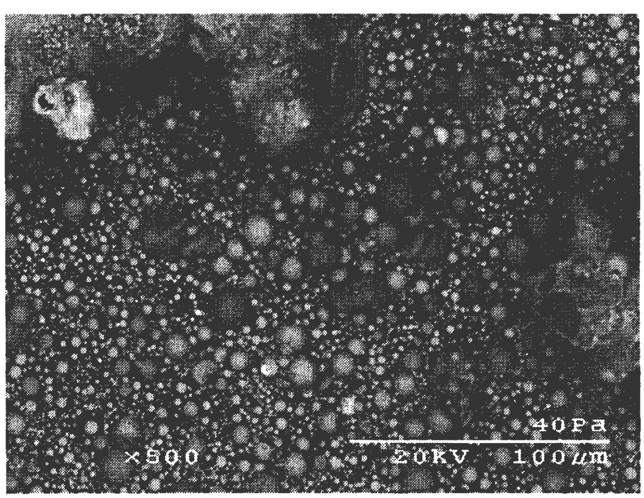

Figure 23. Fly ash particle shape

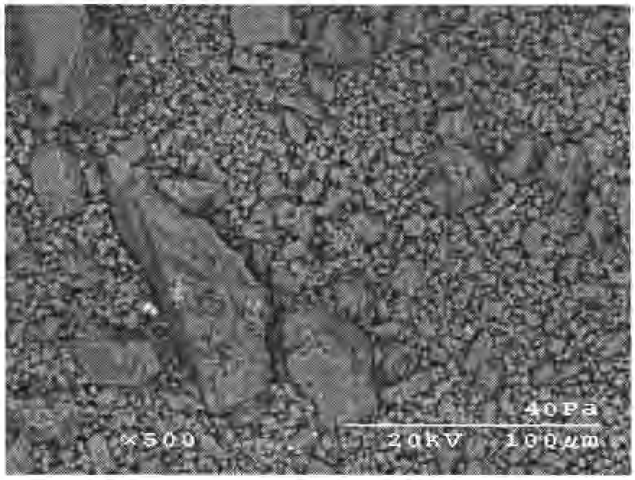

Figure 24. Calcium carbonate particle shape

The densities of the fly ash and calcium carbonate are similar being 2600-2700 kg/m^3 [44]. Average particle size of the two materials is 10-15 µm. Yet when filtered the fly ash filters at 97.32% efficiency and the calcium carbonate at 94.67% efficiency. The shape of calcium carbonate being less spherical than fly ash is resulting in decreased efficiency. This agrees with Shimada et al. in their conclusion of more spherical particles with smoother surfaces having larger adhesion forces due to a reduction in separation distance leading to a larger effective contact area for Van der Waals forces [45].

The shape of the particles also affects the ability of the flowing gas to re-entrain the particles once captured. Irregular particle shapes produce larger drag forces than more spherical shapes, and larger particles have higher drag forces than smaller ones. **Figure 25** displays the affects of boundary layer flow on drag forces for large and small particles. The Reynolds number range for fluid flow in the granular bed is from 100 to

800 indicating laminar flow [46]. Laminar flow is dominated by viscous effects of the flowing gas creating large boundary layers of variable gas velocities near the surface.

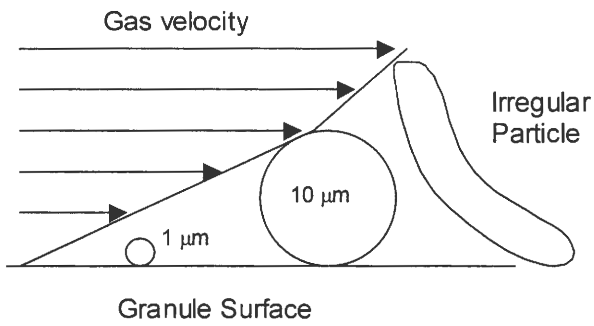

Figure 25. Drag forces on small and large dust particles

The irregular fibrous shape of pyrolysis char and the large particle size as seen in **Figure 20** and **Figure 21** is subjecting the particles to larger gas velocities. The larger gas velocities impingent on the particles is contributing to larger drag forces causing re-entrainment and poor filtration.

Figure 26 shows a fibrous particle approaching a granule collector. The probability of a fiber being collected by interception is depends on fiber orientation at the moment of impact.

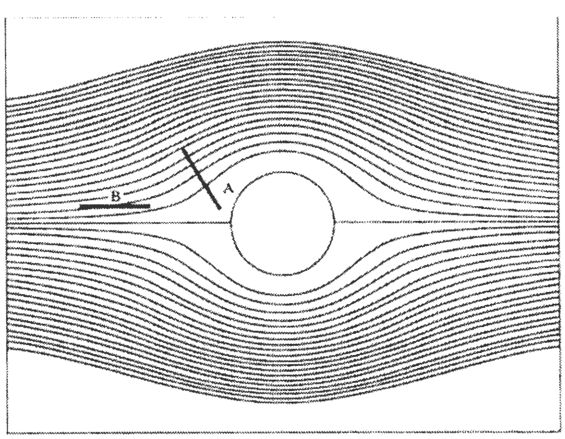

Figure 26. Fibrous particle approaching collector [10]

The orientation of a particle depends on the forces acting on it caused by velocity gradients in the flow field as well as interactions with other particles or granules. Particle A of the figure will have a higher collection efficiency than particle B if they impact the granule in their current orientation [10]. The larger the ratio of length to cross-sectional diameter, the less the collection efficiency will be [10]. Thus the fibrous shape of char causes various impaction orientations that are less efficient in removal than if the particle was spherical.

Surface roughness is similar to particle shape in how it affects granule and particle interactions. The surface roughness affects how the particle interacts with the granular surface as well has how strong the adhesion bonds are once the particle is captured. **Figure 27** shows surface interactions with varying surface roughness of both particle and granule. As surface roughness increases, the contact area between the surfaces decreases.

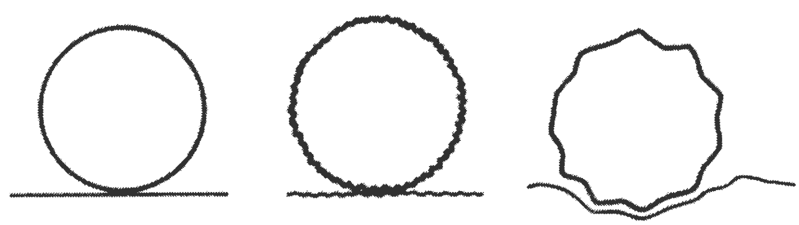

Figure 27. Influence of surface roughness on contact area [30]

When granule or particle roughness increases, it increases the distance between the granule and the adhering particle and also decreases the number of contact points between the two particles. The increased distance causes less mass to be present in the vicinity of attraction and surface area of contact to decrease. These changes in interaction decrease the magnitude of adhesion forces [47]. However, as the surface roughness approaches the average particle dimensions, surface irregularities become insurmountable obstacles and increase the probability of particulate collection [30]. Surface roughness on granular media roughly the size of the dust to be filtered causes turbulent gas flow increasing the collision efficiency and it also causes increased surface contact area and increased adhesion forces [48].

Van der Waals forces are the primary adhesion forces for particle adhesion when electrostatic enhancement forces and surface tension forces of liquids are not present [24]. The Vander Waals forces are dependent on the distance between the surfaces of the two adhering bodies, the particle radius and the material properties. As surface roughness of either body increases or the sphericity decreases, the distance between the interacting surfaces increases and the Van der Waals forces of adhesion decrease. This decrease in adhesion forces allows for easier re-entrainment of particles.

Van der Waals forces are also dependent on the Hamaker constant, which is based on particle composition [10,47,49]. Char is mostly composed of carbon, which has a high Hamaker constant compared to other materials [10]. Van der Waals forces also increase with increasing particle size. Therefore the parameter that is limiting the Van der Waals forces of adhesion for char must be the separation distance between particle and granular surface. Irregular shape and surface roughness of the char is limiting the adhesion forces.

Particle density is also a very important physical property contributing to filtration efficiency. More dense particles have higher moments of inertia and have increased collision efficiency with granular media. The importance of density was compared in a test of calcium carbonate and cornstarch efficiency. Both materials have similar average particle size and shape. The notable difference between the two being density. Calcium carbonate has a density near 2700 kg/m^3 where cornstarch is only 1500 kg/m^3 [44]. The efficiency of the calcium carbonate is 94.67% while the cornstarch is only 91.15%. Therefore a decrease in density is decreasing the collision efficiency of the dust particles as they traverse the granular bed for a given particle size. Char from oak has a density of 560 kg/m^3 [44]. This provides additional explanation why a test of char particles of similar size as fly ash, calcium carbonate and starch do not filter as efficiently as any of the more dense materials.

Tardos notes that large particles favor filtration by a dust cake layer that builds up in the filter, and small particles favor filtration in relatively deep beds of clean filter media [50]. The formation of a dust coating or layer decreases adhesion forces between dust and granule by increasing the distance between them; however the deposited dusts acts like a "landing pad" for incoming particles and reduces particle bounce [10]. Smaller particles are less likely to rebound and thus cleaner granules with larger adhesion forces will have higher efficiencies for these small particles. Lippert, Shi and Brown have observed dust cake formation visually, and this phenomenon should be considered as a way to increase filtration efficiency of larger char particles that are experiencing rebound and re-entrainment from the granular surfaces and penetrating the granular bed [41, 8, 39].

5. CONCLUSIONS

The moving bed granular filter design is capable of reaching high efficiencies with an optimal design of the interfacial and downcomer regions for fly ash filtration. Both regions affect the overall filtration efficiency of the MBGF system. Superficial gas velocities in either the downcomer or interfacial regions may be high compared to typical barrier filtration velocities and still achieve high levels of filtration, but both regions cannot have high superficial velocities at the same time.

The effect of reducing the granular media size to 2 mm for the filtration of fly ash showed little improvement over the 4 mm granules. The change in granule size was more significant for the larger char particles. The reduction in granule size should have larger effects for the larger dust particles because of the reduction in interstitial void size is of the same order of magnitude as the dust size itself. This reduction in void size leads to more sieving filtration for the large char particles while the small fly ash particles do not experience more sieving filtration.

The adsorption model application to the filtration of fly ash allows the interfacial efficiency to be distinguished from the downcomer bed efficiency of the filter. This is a useful model to aid future researchers in measuring interfacial efficiency to investigate optimizing filtration in this region. The model is best suited to mono-disperse dust that has constant layer efficiency and the filter is operated in filtration modes where particle bounce and re-entrainment is not dominating penetration. Applications where disperse dust is being characterized is better described by poly-disperse models based on mass fractions and layer efficiencies for given particle size ranges.

Char from the pyrolysis of oak does not filter as well as coal-derived fly ash due to smaller adhesion and impaction probabilities. Large length to cross-sectional diameter ratios increases the drag forces on the char particles causing re-entrainment. Char particles also have large surface irregularities that cause a decrease in contact area. This decrease in contact area and increase in particle separation distance decreases the adhesion forces between particle and collector. The decreased adhesion force and increased drag force increases the particle penetration through the granular bed.

Char particles are less dense than fly ash decreasing the probability of impact with the granular surface. More dense particles have higher inertia than less dense particles of the same size. The increase in inertia causes the more dense particles to deviate from the gas flow patterns and impact granular surfaces more readily. This increase in collision efficiency as the particles traverse the granular bed increases the collection probability.

The dimensionless Modified Stokes number characterizes the effects of particle size and density as well as gas velocity and viscosity. Char particles have Modified Stokes numbers that are a factor of two larger than those of fly ash. These high numbers verify high particle kinetic energies as well as large particle drag forces causing reduced adhesion probability.

To increase the filtration of char particles, the gas velocity must be reduced to decrease the kinetic energy and drag forces. A pre-filtration device such as a cyclone before the MBGF system that removes the large particles may be desired to reach higher levels of overall efficiency. The MBGF system filters small particles well and could be used as a polishing filter. If pre-filtration is undesired, then optimization of other filtration mechanisms such as cyclonic action, sieving and "cake" filtration should be utilized.

Possible areas for future investigation include the use of different granular materials with properties more conducive to filtration. Coatings of granular materials such as with high temperature paint could increase the tackiness. Granular media of softer materials decrease the probability of particle bounce and subsequent re-entrainment.

It may also be valuable to design a filter that has a variable area downcomer to allow for varying flow conditions to optimize single particle filtration efficiencies. By varying the flow conditions within the downcomer, dust to be filtered will flow through the filter and reach different velocity zones where optimal filtration occurs for each different particle size within the distribution.

BIBLIOGRAPHY

1. Roadmap for Biobased Technologies in the United States. <http://www.bioproducts-bioenergy.gov/pdfs/FinalBiomassRoadmap.pdf>. Online September 26, 2003.
2. Vision for Bioenergy and biobased products in the United States. <http://www.bioproducts-bioenergy.gov/pdfs/BioVision_03_Web.pdf>. Online September 26, 2003.
3. Soo, Saw-Choon. 2002. Empirical model optimization of a moving bed granular filter for particulate removal. M.S. Thesis. Iowa State University.
4. Bridgewater, A. V. et al. 2001. An Overview of Fast Pyrolysis. In Progress in Thermochemical Biomass Conversion. Volume 2. 977-997. Blackwell Science Ltd.
5. Scahill, J. et al. Removal of Residual Char Fines from Pyrolysis Vapors by Hot Gas Filtration. Online: November 8, 2003. <http://www.eere.energy.gov/biopower/bplib/library/removalresidualcharfines.pdf>.
6. Diebold, J.P. et al. 1994. Hot-gas filtration to remove char from pyrolysis vapors produced in the vortex reactor at NREL. Specialists' Workshop on Biomass Oil Properties and Combustion, Estes Park, CO, September 26-28.
7. Tien, C. 1989. Granular Filtration of Aerosols and Hydrosols. Butterworths.
8. Shi, Huawei. 2002. Similitude modeling and experiments on a moving bed granular filter. M.S. Thesis. Iowa State University.
9. Miyamoto, S. et al. 1975. Filtration of airborne particulates by gravel filters: II collection efficiency and pressure drop in filtering fume. Journal of the Air Pollution Control Association, Vol. 24, No. 1, pp. 40-43.
10. Brown, R.C. 1993. Air Filtration An Integrated Approach to the Theory and Applications of Fibrous Filters. Pergamon Press.
11. Freidlander, S.K. 1977. Smoke, Dust, and Haze. John Wiley & Sons, NY.
12. Flagan, Richard C., John H. Seinfeld. 1988. Fundamentals of Air Pollution Engineering. Prentice-Hall Inc. Englewood Cliffs, New Jersey.

13. Zevenhoven, C. A. P. et al. 1993. Moving granular bed filtration with electrostatic enhancement for high-temperature gas clean-up. Filtration and Separation. 30(6). 550-553.

14. Kalinowski, T. et al. 1981. Aerosol Filtration by a Cocurrent Moving Granular Bed: Penetration Mechanisms. Environment International. 6:379-386.

15. Saxena, S. C. et al. 1985. Particulate removal from high temperature, high-pressure combustion gases. Progress in Energy Combustion Science. 11(3):193-251.

16. Jordan, S. et al. 1988. Experiences with crossflow granular bed filter. Chemical Engineering Technology. 60(1): 34-35.

17. Tsubaki, J. et al. 1988. Gas filtration in granular moving beds-an experimental study. The Canadian Journal of Chemical Engineering. 66:271-275.

18. Kalinowski, T. et al. 1983. Aerosol Filtration by a Cocurrent Moving Granular Bed: Penetration Theory. Environmental Science and Technology. 17:20-26.

19. Otani, Y. et al. 1990. Collection performance of moving granular bed filters. Proc. International Aerosol Conference. 733-735.

20. Toyama, Shigeki, 1970/71. The flow of granular materials in moving beds. Powder Technology. 4:214-220.

21. Takahashi, H. et al. 1973. Flow profile and void fraction of granular solids in a moving bed. Powder Technology. 7: 205-214.

22. Pinson, D. et al. 1997. Powder Entrapment in a Multi-Phase Flow Packed Bed. In Processing and Handling of Powders and Dusts. Edited by T.P.Battle and H. Henein. The Minerals, Metals & Materials Society. 257-267.

23. Guillory, J.L. Filtration performance of a moving bed granular filter: Experimental cold flow data Proceedings of the Fifth International Conference on Fluidized Bed Combustion. December 12-14, 1977. Vol. III. Developmental Activities.

24. Davies, C. N., 1973. Air Filtration. Academic Press Inc.

25. Henriquez, V. et al. 1997. Hot gas filtration using a moving bed heat exchanger-filter. Chemical Engineering and Processing. 36: 353-361.

26. Kuo, J.T. et al. 1998. Granular Bed Filter Technology. Proc. Nat. Sci. Council ROC (A). 22:17-34.

27. Peukert, W. et al. 1991. Influence of temperature on particle separation in granular bed filters. Powder Technology. 68: 263-270.

28. Gutfinger, C. et al. 1980. Granular bed filter for high-temperature particulate removal. VDI-Berichte Nr. 363: 83-86.

29. Dahneke, B. 1971. The capture of aerosol particles by surfaces. J. Coll. Interface Science. 37(2): 342-353.

30. Visser, J. 1978. Colloid and other forces in particle adhesion and particle removal. In Deposition and Filtration of Particles from Gases and Liquids. 121-142. The Society of Chemical Industry.

31. Knettig, P. et al. 1974. Capture of monodispersed aerosol particles in a fixed and in a fluidized bed. Canadian Journal of Chemical Engineering. 52:703-706.

32. Daugaard, D. E. 2003. The transport phase of pyrolytic oil exiting a fast fluidized bed reactor. Ph.D. Dissertation. Iowa State University.

33. Nunez, J. S. 2002. Evaluation of a moving bed granular filter in conjunction with a biomass gasifier. M.S. Thesis. Iowa State University.

34. Herdan, G. 1953. Small Particle Statistics. Elsevier Publishing Company.

35. Wheeler, A. 1969. Performance of fixed-bed catalytic reactors with poison in the feed. Journal of Catalysis. 13:299-305.

36. Amundson, N.R. 1948. A note on the mathematics of adsorption in beds. Journal of Physical Chemistry. 52:1153.

37. Gal, E. et al. 1985. A Study of inertial effects in granular bed fliltration. AlChE Journal. 31(7): 1093-1104.

38. Brown, Robert C. et al. 2003. Similitude Study of a Moving Bed Granular Filter. Powder Technology. In Review.

39. Brown, R. C. et al. 2000. Design of a moving bed granular filter for biomass

gasification. Proceeding of the Progress in Thermochemical Biomass Conversion Conference. Tyrol, Austria. September 17-22.

40. Thambimuthu, K.V. et al. 1978. Aerosol filtration in fixed granular beds. In Deposition and Filtration of Particles from Gases and Liquids. 107-120. The Society of Chemical Industry.
41. Lippert, T. E. et al. 1981. Testing and verification of granular bed filters for removal of particulates and alkalies: High Temperature, High Pressure Particulate and Alkali Control in Coal Combustion Process Streams. Proceedings U.S. DOE Contractors' Meeting. Conf-810249. 471-489.
42. Yoshida, H. et al. 1985. A new correlation of the initial collection efficiency of granular aerosol filtration. AlChE Journal. 31(10): 1752-1754.
43. Wang, H. et al. 1987. Comparative bounce properties of particle materials. Aerosol Science and Technology. 7:285-299
44. Densities of common material. < http://admin.engr.wisc.edu/quest/OPS/ops98.htm>. Online: March 16, 2004.
45. Shimada, Y. et al. 2002. Development of an apparatus for measuring adhesive force between fine particles. KONA. 20:223-229.
46. Munson, B.R. et al. 2002. Fundamentals of Fluid Mechanics. Fourth Edition. John Wiley and Sons, Inc.
47. Ranade, M.B. 1987. Adhesion and removal of fine particles on surfaces. Aerosol Science and Technology. 7:161-176.
48. Purchas, D.B. 1997. Handbook of Filter Media. Elsevier Advanced Technology.
49. Mullins, M.E. 1992. Effect of geometry on particle adhesion. Aerosol Science and Technology. 17:105-118.
50. Tardos, G. I. 1998. Separation of airborne dust in deep-bed filtration. Advances in Aerosol Filtration. Edited by Kvestoslav R. Spurny. 241-258. Lewis Publishers.

Appendix A. Efficiency Calculation

m_{HEPA} is the weight of the dust collected by the HEPA filter from the effluent of the MBGF system. m_{out} is the amount of fly ash removed by the granular filter and m_{in} is the amount of fly ash injected into the filter. η is the measured efficiency. A typical test yielded the following results:

$m_{HEPA} = 23.90$ grams, $m_{in} = 926.88$ grams

$m_{out} = m_{in} - m_{Hepa} = 902.98$

$$\eta = \frac{m_{in} - m_{out}}{m_{in}} = 0.9742$$

$$U_{eff} = 0.9472 \cdot \sqrt{(\frac{0.4359}{902.98})^2 + (\frac{0.3082}{926.88})^2} = 0.00057$$

Therefore the efficiency for the test is reported as 97.42 ±0.06%.

Appendix B. Variable Area Flowmeter Calibration

The variable area flow meter was calibrated using an Alicat Scientific model MC-500SLPM-D(N2) mass flow meter. The mass flow meter was set at different desired flow rates using compressed nitrogen for the gas. The pressure at the exit of the variable area flow meter and its readings were recorded for each of the flow settings. The actual flow rate for air was then calculated using a correction for the specific gravity and the pressure as follows:

$$Rotameter(CFM) = \sqrt{0.967 * \frac{406.5}{406.5 + pressure}} * MassFlowMeter(SCFM)$$

Mass Flow Meter (SCFM)	Rotameter (SCFM)	Pressure (in H2O)	Rotameter (CFM)
2.50	1.90	0.40	2.46
5.00	4.50	1.30	4.91
7.50	6.70	2.80	7.35
10.00	9.00	5.00	9.77
12.50	11.60	7.85	12.18
15.00	13.90	11.30	14.55
17.50	16.10	15.80	16.88
9.18	8.50	4.30	8.98
8.48	8.20	3.60	8.30
7.77	7.30	2.95	7.61

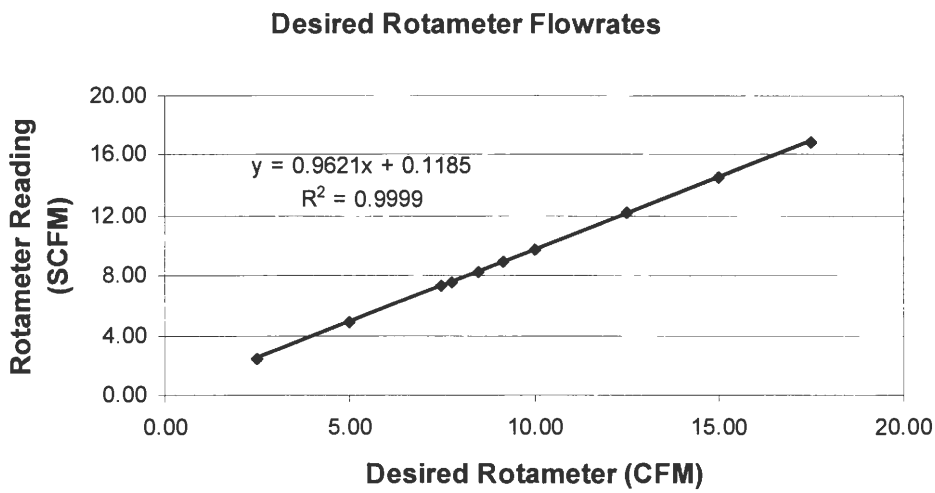

Appendix C. Uncertainty Analysis

Uncertainty from measurements and calculations depends on the equipment and the type of equation used. The uncertainty equations for addition and multiplication calculations are as follows:

Addition: $y = Ax_1 + Bx_2$ $\quad U_y = \sqrt{(A \cdot U_1)^2 + (B \cdot U_2)^2}$

Multiplication: $y = \dfrac{x_1^{\,m} \cdot x_2^{\,n}}{x_3^{\,k}}$ $\quad U_y = y \cdot \sqrt{(m\dfrac{U_{x1}}{x_1})^2 + (n\dfrac{U_{x2}}{x_2})^2 + (k\dfrac{U_{x3}}{x_3})^2}$

y = calculated value; U_y=uncertainty in the value y; x_i = measured quantities used to calculate y; and A, B, m, n and k are constants

The uncertainty in the calculation of efficiency comes from error in the scale used to weigh the dust, and it also comes from dust that is not measured because it remains adhered to the sides of the solids feeder and the effluent Hepa filter box. A paper towel was used to wipe the adhered dust from the feeder and the effluent box to determine the uncertainty of unmeasured dust. The uncertainty of the dust adhered to the solids feeder is ±0.30 grams. The uncertainty of the dust adhered to the effluent box is also ±0.30 grams. The uncertainty of the scale is ±0.05 grams. A sample calculation follows:

Uncertainty of fly ash injected: $U_{in} = \sqrt{0.3^2 + 0.05^2 + 0.05^2} = 0.3082$

Uncertainty of fly ash effluent: $U_{vac} = \sqrt{0.3^2 + 0.05^2 + 0.05^2} = 0.3082$

Uncertainty of fly ash removed: $U_{rem} = \sqrt{0.3082^2 + 0.3082^2} = 0.4359$

Uncertainty of efficiency: $U_{eff} = Efficiency \cdot \sqrt{(\dfrac{U_{rem}}{A})^2 + (\dfrac{U_{in}}{B})^2}$

Appendix D. Granule Feed Rate Calibration

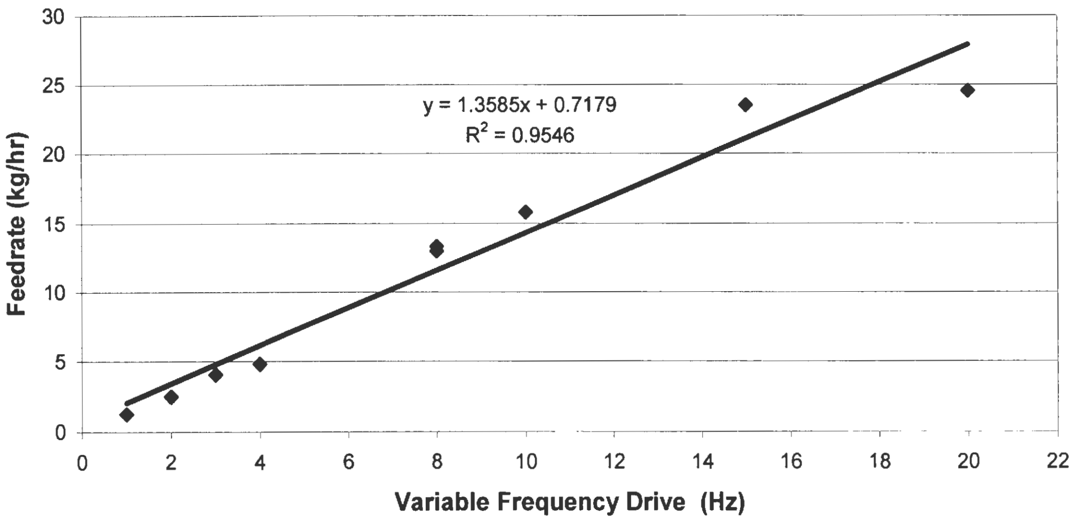

Appendix E. 95% Confidence Interval Calculation

Confidence interval calculation is useful in evaluating how close a calculated average based on test results is compared to the actual average. It is also useful in comparing two data sets to test for differences between the sets. The testing outcomes have a normal distribution about the average. A t-distribution is then appropriate for calculating confidence intervals. T-tests for differences are also valid since they are robust to differences in standard deviations between tests as long as the sample sizes are about the same. The t-distribution table used to obtain values for the calculations here is located in The Statistical Sleuth-A Course in Methods of Data Analysis, Second Edition, by Fred L. Ramsey and Daniel W. Schafer.

		Example:
		97.42
		97.18
		97.37
Sample size (n)		3
Degrees of Freedom (df)	$n-1$	2
Average ($\bar{Y}$)	$\frac{\sum Y_i}{n}$	97.32
Standard Deviation (sd)	$\sqrt{\frac{\sum (Y_i - \bar{Y})^2}{n-1}}$	0.1266
t-statistic (t_{df})	2.403	2.403
Standard Error (SE)	$\frac{sd}{\sqrt{t_{df}}}$	0.0731
Tolerance (%)	$\pm$	0.3146

Appendix F. Fluidization Velocity Calculation

The fluidization velocity of a material is calculated by placing filling a pipe of known diameter with a few inches of the material. A pressure drop within the material is taken as the controlled gas flow rate is increased. The transistion where the pressure drop no longer increases as the flow rate increases is the location of minimum fluidization. This location is can also be noted by the onset of slight material movement. The known gas flow rate at this transistion and the dimensions of the pipe are then used to calculate the superficial velocity at the point of minimum fluidization. Figure 20 and the calculation for the nominal 4 mm granules is presented.

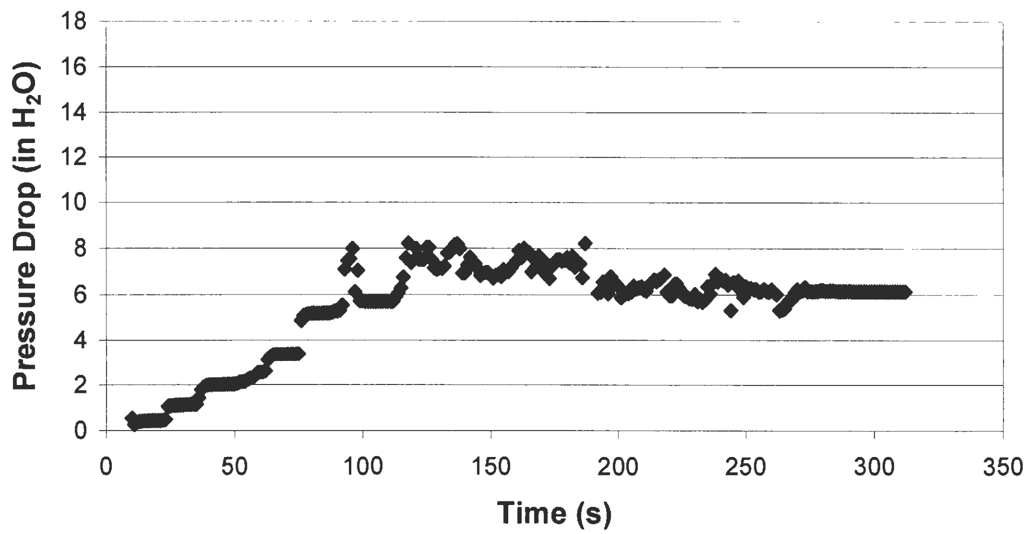

Pipe Diameter: $D = 2 \cdot inches$ Gas Flow Rate: $Q = 7 \cdot cfm$

Superficial Velocity: $U = \dfrac{Q}{A}$

Fluidization Velocity: $U = \dfrac{7\,ft^3}{\min} \cdot \dfrac{1}{\pi \cdot 2^2 in^2} \cdot \dfrac{144 in^2}{ft^2} \cdot \dfrac{\min}{60\sec} \cdot \dfrac{m}{3.28 ft} = 1.63 \dfrac{m}{\sec}$

Appendix G. Gas Velocity Calculation

The interfacial area is the area where the dust-laden gas first encounters the granular media. The superficial velocity is the velocity of the gas inside the downcomer if there was no granular media present. Gas velocity is then calculated based on gas flow rate and area. The formula is as follows:

$$U = \frac{Q}{A}$$

U: gas velocity

Q: gas volumetric flow rate

A: cross-sectional area through which gas flows

For the 6-inch nominal downcomer, the interfacial gas velocity is as follows with a volumetric flow rate of 20 cfm:

$$Q = \frac{20\,ft^3}{\min} \cdot \frac{\min}{60\sec} \cdot \frac{0.3048^3 m^3}{ft^3} = 0.009\frac{m^3}{\sec}$$

$$A = \frac{\pi\left(7.5^2 - 6.625^2\right)in^2}{4} \cdot \frac{0.0254^2 m^2}{in^2} = 0.00626\ m^2$$

$$U = \frac{0.009\frac{m^3}{\sec}}{0.00626^2} = 1.44\frac{m}{\sec}$$